doi.org/10.26434/chemrxiv.14687331.v1

Complete Deconstruction of SF6 by an Aluminium(I) Compound

Daniel Sheldon, Mark Crimmin

Submitted date: 27/05/2021 • Posted date: 28/05/2021

Citation information: Sheldon, Daniel; Crimmin, Mark (2021): Complete Deconstruction of SF6 by an Aluminium(I) Compound. ChemRxiv. Preprint. https://doi.org/10.26434/chemrxiv.14687331.v1

The room-temperature activation of SF_6, a potent greenhouse gas, is reported using a monovalent aluminium(I) reagent to form well-defined aluminium(III) fluoride and aluminium(III) sulfide products. New reactions have been developed to utilise the aluminium(III) fluoride and aluminium(III) sulfide as a nucleophilic source of F^- and S^{2-} for a range of electrophiles. The overall reaction sequence results in the net transfer of fluorine or sulfur atoms from an environmentally detrimental gas to useful organic products.

File list (2)

Complete Deconstruction of SF_6 by an Aluminium(I) Compound

Daniel J. Sheldon, Mark R. Crimmin*

Molecular Sciences Research Hub, Imperial College London, 82 Wood Lane, White City, London, W12 0BZ, UK.

The room-temperature activation of SF_6, a potent greenhouse gas, is reported using a monovalent aluminium(I) reagent to form well-defined aluminium(III) fluoride and aluminium(III) sulfide products. New reactions have been developed to utilise the aluminium(III) fluoride and aluminium(III) sulfide as a nucleophilic source of F^- and S^{2-} for a range of electrophiles. The overall reaction sequence results in the net transfer of fluorine or sulfur atoms from an environmentally detrimental gas to useful organic products.

Sulfur hexafluoride (SF_6) is widely used as an electrical insulating gas in circuit breakers.[1] SF_6 possesses unique chemical and physical inertness and excellent thermal conductivity; properties that result from its high dielectric constant, high heat capacity and high density.[1–3] However, SF_6 is a potent greenhouse gas with a global warming potential (GWP_{100}) 23,900 times greater than CO_2 and a long atmospheric lifetime of 3200 years.[4–7] As a result, its emission is restricted through the Kyoto protocol as one of the six most prominent greenhouse gases.[6–8] Specific attention has been directed towards its control as in many cases there are no suitable alternatives or drop-in replacements for SF_6.[4,6,9] Typical methods for its destruction are energy intensive and often produce toxic and corrosive products.[10–12] Efficient methods for recycling or destroying SF_6 are therefore highly sought after.[13]

A challenge remains to transform SF_6 into non-toxic, high-value compounds under mild reaction conditions.[12] Not only does this offer an attractive method for its depletion, but it opens up the potential to use SF_6 as a source of S and F atoms through the deconstruction of this molecule to its elemental components. In particular, there has been recent interest in using SF_6 as a fluorinating agent in organic synthesis. Fluorinated building blocks are increasingly crucial in the pharmaceutical, agrochemical and materials industries, where fluorine substitution is used to improve the quality and efficiency of new products.[14–16]

The activation and chemical deconstruction of SF_6 has been achieved with strong reducing agents or low-valent transition metal complexes.[9,17–26] The latter approach results in the formation of transition metal fluorides and sulfides. Metal-free approaches have also been reported in which strong nucleophiles directly attack SF_6.[27] In recent years, these synthetic approaches have been developed further and reactions that

allow the onwards use of the fluorine content of SF_6 in organic synthesis have been targeted. Particular attention has been given to the use of SF_6 in the deoxyfluorination of alcohols.[18,28–34] In one example, Braun and co-workers developed a photochemical protocol in which SF_6 is reduced by an NHC to form a difluoroimidazolidine, which was then successfully applied in the deoxyfluorination of a range of alcohols.[30]

For some time we have been interested in using main group nucleophiles to activate the C–F bonds in environmentally persistent fluorocarbons.[35–42] Herein we report the extension of this methodology to the rapid, room temperature activation of SF_6 by a monovalent aluminium(I) species. This reaction results in the complete deconstruction of SF_6 to its reduced elemental components, forming well-defined aluminium(III) fluoride and sulfide products. The fluoride species can be used as a nucleophile in onward synthesis, while the sulfide species is shown to act as a sulfide source in the formation of a heterocycle, thus allowing the elemental fluorine and sulfur content of SF_6 to be re-used.

An excess of sulfur hexafluoride (1 bar) was added to a C_6D_6 solution of [{(ArNCMe)$_2$CH}Al] (**1**, Ar = 2,6-di-isopropylphenyl). The red solution rapidly turned pale yellow. Monitoring the reaction by ^{1}H and ^{19}F NMR spectroscopy revealed the complete consumption of **1** and the formation of [{(ArNCMe)$_2$CH}AlF$_2$] (**2**) within 15 min at 22°C (Scheme 1).

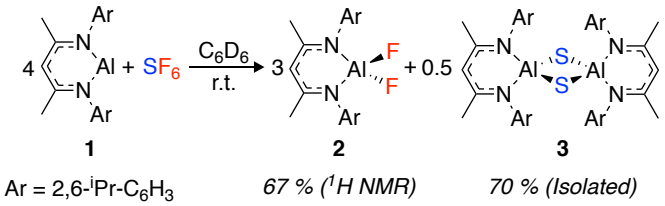

Scheme 1: Reaction scheme for SF_6 activation by **1**. ^{1}H NMR yields are reported against a ferrocene internal standard..

2 is a known compound and the data match that reported in the literature.[37] Although no further products were detected by NMR spectroscopy, the reaction was accompanied by the production of a colourless precipitate, suggesting the formation of an insoluble by-product. Repeating the reaction with slow diffusion of the SF_6 into a C_6D_6 solution of **1** led to the formation of single crystals of the insoluble product suitable for X-ray diffraction. The side-product was determined as [{(ArNCMe)$_2$CH}Al(μ-S)]$_2$ (**3**) (Scheme 1).[43] **3** is also a known compound, and crystallised as a polymorph (monoclinic, C2/c) of a previously reported structure (monoclinic, C2/m). Crystalline samples of **3** were found to be insoluble in common laboratory solvents.

The mechanism for SF_6 activation was investigated by DFT calculations (Figure 1). The reaction sequence is likely initiated by nucleophilic attack of **1** at a fluorine atom of SF_6, proceeding *via* **TS-1** ($\Delta G_1^{\ddagger}$ = 10 kcal mol^{-1}), to give **2** and SF_4 (**Int-1**). A further equivalent of **1** then reacts with SF_4 in a similar nucleophilic manner *via* **TS-2** ($\Delta G_2^{\ddagger}$ = 11 kcal mol^{-1}) to form SF_2 and **2** (**Int-2**). SF_4 possess a see-saw structure where the axial and equatorial fluorine atoms are inequivalent. The calculations suggest that the most favourable pathway involves attack of **1** at the equatorial fluorine of SF_4 as this is the most electrophilic (least electronegative) site. Another equivalent of **1** then reacts in a similar fashion with SF_2 *via* **TS-3** ($\Delta G_3^{\ddagger}$ = 11 kcal mol^{-1}) to form **Int-3**. **Int-3** is subsequently attacked by a final equivalent of **1**, leading to **Int-4** *via* **TS-4** ($\Delta G_4^{\ddagger}$ = 3 kcal mol^{-1}). A rearrangement to form the experimentally observed products **2** and **3** is calculated to be thermodynamically feasible. When following the reaction by NMR spectroscopy, no reaction intermediates could be detected and the reaction proceeds to completion within 15 minutes at room temperature. These observations are consistent with the small activation barriers calculated for these elementary steps.

Numerous mechanistic analyses of SF_6 activation propose a first step involving single electron transfer to SF_6 from a transition metal, alkali metal or photocatalyst.[9,19,23,25,28–30] Dielmann and co-workers have proposed an alternative mechanism involving nucleophilic attack at the fluorine atom of SF_6 by a strongly nucleophilic phosphine, in a pathway similar to the one calculated here.[27]

NBO analysis of the transition states was carried out. **TS-1**, **TS-2** and **TS-3** are calculated to involve the nucleophilic attack of **1** at a fluorine atom of SF_x (x = 6, 4, 2). The *NPA* charges show a trend of increasing negative charge at the sulfur atom as the maxima associated with the transition state is traversed, and conversely an accumulation of positive charge at aluminium. This implies electron density is transferred from aluminium to sulfur, consistent with nucleophilic attack, rather than a fluoride abstraction mechanism (see ESI for NBO data). Wiberg Bond Indices are consistent with a decrease in the S–F bond order in **TS-1** relative to SF_6 itself (ESI Table S3).

An IRC calculation connects **TS-1** directly to **2** and SF_4 (**Int-1**), where a second fluorine transfer has also occurred. This suggests that the second fluorine transfer step is a barrierless process somewhere on the pathway between **TS-1** and **Int-1**. A very similar process is found for **TS-2**. Second-order perturbation analysis of **TS-1** reveals donation of electron density from the aluminium lone pair into σ*(S–F) (17 kcal mol^{-1}), with simultaneous donation of electron density from the same fluorine atom into the empty p-orbital of the aluminium atom (14 kcal mol^{-1}). Similar donor-acceptor interactions, albeit of slightly different magnitudes are found for **TS-2**, **TS-3** and **TS-4**.

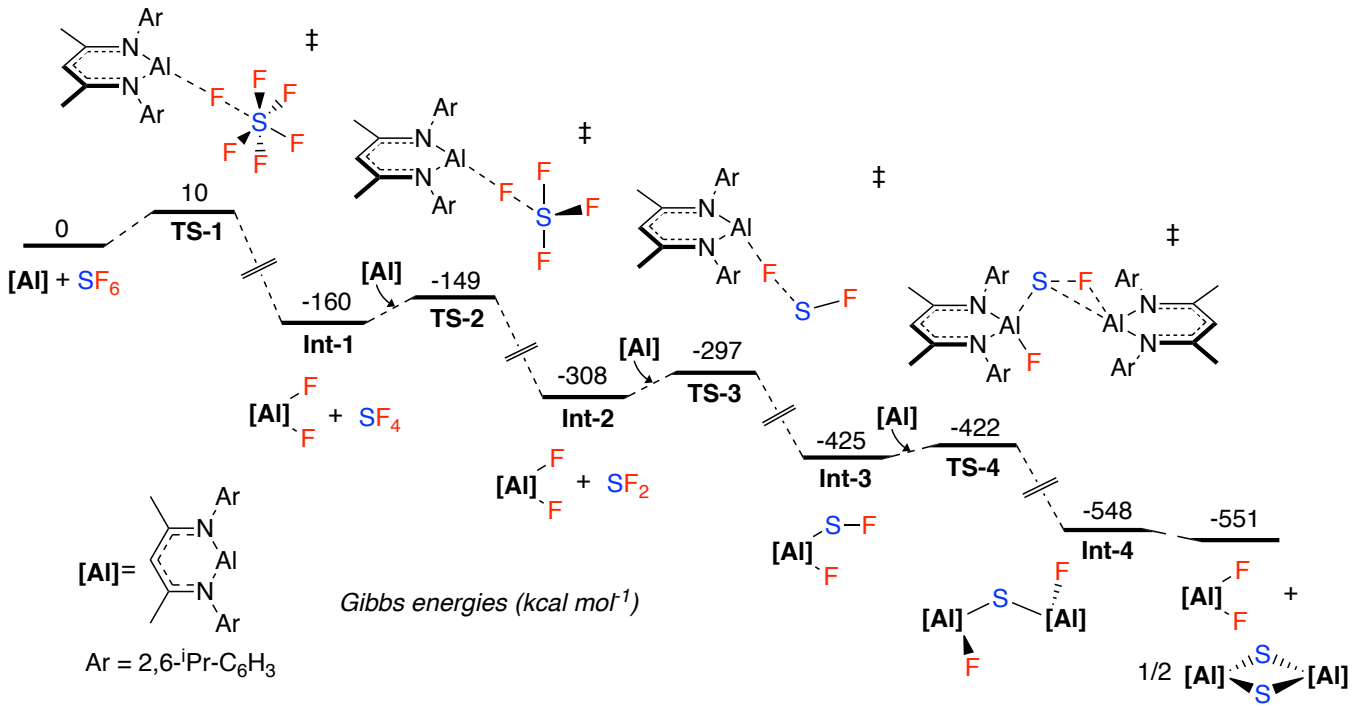

Fig 1: Calculated potential energy surface for SF_6 activation. The M06-2X functional was used with a hybrid basis set, 6-31g**(C,H)/6-311+g*(N,F,S). The SDDAll pseudopotential was used for Al. Dispersion and solvent effects were included *via* single-point corrections, using Grimme's D3 correction for dispersion and the PCM (solvent=benzene) model for solvent.

ETS-NOCV calculations were performed to further probe the postulated nucleophilic attack mechanism.[44] The largest contributor ($\Delta\rho_1$) to the orbital interaction (ΔE_{orb}) for **TS-1**, **TS-2** and **TS-3** involves donation from the aluminium lone pair to σ* (S–F) (Figure 2).

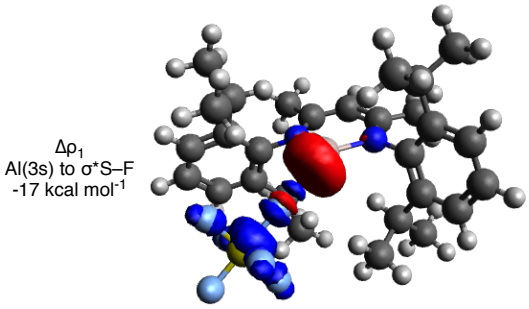

Fig 2: ETS-NOCV deformation density plot for **TS-1**. Charge flow is from red to blue.

It is evident that attack of the aluminium occurs at the fluorine atom of the S–F bond. Along with the orbital interactions discussed, this is likely also due to the electrostatic interaction between Al and F (see ESI for *NPA* charges), and the fluorophilic nature of aluminium. There is a contrast here to halocarbon reactivity where 'frontside' S_N2X attack at the halogen atom is rare, although has been proposed in some recent examples with other fluorophilic nucleophiles.[38,45,46] We were interested in the utility of the fluorinated aluminium species **2** as a nucleophile for onward synthesis. Organoaluminium fluorides have been the subject of previous reviews.[47,48] The use of these compounds as a nucleophilic source of fluorine is very rare owing to the thermodynamic stability of the Al–F bond.[49,50] We report here a fluoride metathesis reaction of **2** with various electrophiles (Figure 3).

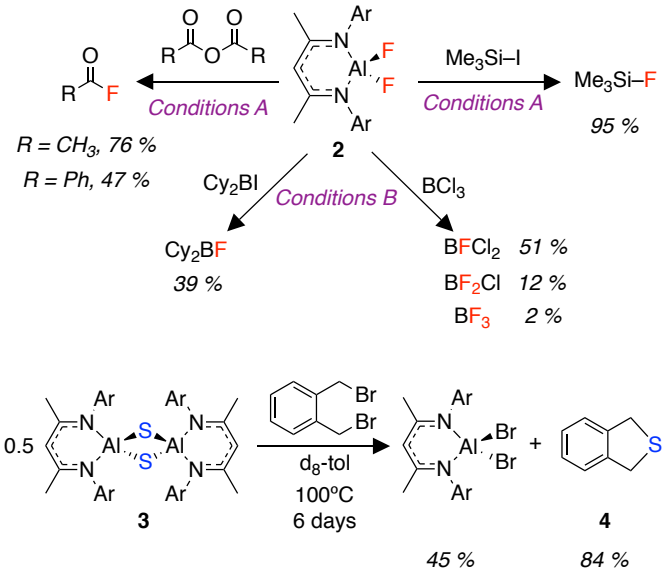

Fig 3: Fluoride and sulfide transfer reactions. Conditions A: heat at 150°C for 16 hours in *m*-xylene solvent. Conditions B: room temperature for 10 minutes in *m*-xylene solvent. 10 equiv. of electrophile used for all the above reactions. Yields are determined by quantitative ^{1}H or ^{19}F NMR spectroscopy against a ferrocene, 1,3,5-trimethoxybenzene or 1,2-difluorobenzene internal standard.

Reaction of **2** with organic anhydrides resulted in the formation of acyl fluorides. Acyl fluorides are becoming increasingly important and valuable fluorinating agents due to their unique balance of stability and reactivity.[51–54] Furthermore, the reaction of **2** with trimethysilyl iodide produces trimethylsilyl fluoride, a silylating agent for ketones, alcohol, terminal alkynes and various lithiated precursors.[55–59] **2** also reacted with BCl_3 to produce a series of commercially relevant Lewis acids.[60,61] Finally, despite its lack of solubility, we were able to demonstrate the transfer of sulfide (S^{2-}) from **3** to α,α′-dibromo-*o*-xylene to form the sulfur heterocycle **4** (Figure 3).[62] These fluoride (F^-) and sulfide (S^{2-}) transfer reactions represent a formal re-use of the atoms derived from SF_6, and thus the overall reaction sequence describes the transfer of fluorine and sulfur from a potent greenhouse gas to highly useful organic products.

In conclusion, we have developed a metal-free process to deconstruct the potent greenhouse gas SF_6 to its elemental components (F^- and S^{2-}) using a monovalent aluminium(I) compound under ambient conditions. The aluminium(III) fluoride and sulfide products of the reaction are well-defined and easy to separate by virtue of their differing solubilities. We have undertaken DFT calculations to propose a viable pathway for SF_6 activation through nucleophilic attack by the Al(I) fragment at the σ*(S–F) orbital of an S–F bond. We have demonstrated the utility of the aluminium difluoride product (**2**) as a nucleophilic source of fluorine for organic substrates, and we have shown the ability of **3** to transfer it's sulfide content. Overall, the complete activation of SF_6 to its elemental components has been developed in a system where the fluorine and sulfur content can be re-used in the synthesis of valuable compounds.

We are grateful to ERC for generous funding (Fluorofix:677367), to the EPSRC and Imperial College London for DTP studentship funding (Daniel Sheldon), and Richard Kong is thanked for help with crystallography.

References

1 L. G. Christophorou, J. K. Olthoff and R. J. Van Brunt, *IEEE Electr. Insul. Mag.*, 1997, **13**, 20–24.
2 J. R. Case and F. Nyman, *Nature*, 1962, **193**, 473.
3 K. Seppelt, *Chem. Rev.*, 2015, **115**, 1296–1306.
4 M. Rigby, J. Mühle, B. R. Miller, R. G. Prinn, P. B. Krummel, L. P. Steele, P. J. Fraser, P. K. Salameh, C. M. Harth, R. F. Weiss, B. R. Greally, S. O'Doherty, P. G. Simmonds, M. K. Vollmer, S. Reimann, J. Kim, K.-R. Kim, H. J. Wang, J. G. J. Olivier, E. J. Dlugokencky, G. S. Dutton, B. D. Hall and J. W. Elkins, *Atmos. Chem. Phys.*, 2010, **10**, 10305–10320.
5 M. Maiss and C. A. M. Brenninkmeijer, *Environ. Sci. Technol.*, 1998, **32**, 3077–3086.
6 K. S. Betts, *Environ. Sci. Technol.*, 1998, **32**, 487A-488A.
7 G. P. Stiller, T. von Clarmann, M. Höpfner, N. Glatthor, U. Grabowski, S. Kellmann, A. Kleinert, A. Linden, M. Milz, T. Reddmann, T. Steck, H. Fischer, B. Funke, M. López-Puertas and A. Engel, *Atmos. Chem. Phys.*, 2008, **8**, 677–695.
8 A. A. Lindley and A. McCulloch, *J. Fluor. Chem.*, 2005, **126**, 1457–1462.
9 L. Zámostná and T. Braun, *Angew. Chem., Int. Ed.*, 2015, **54**, 10652–10656.
10 R. Kurte, H. M. Heise and D. Klockow, *J. Mol. Struct.*, 1999, **480–481**, 211–217.
11 C.-H. Tsai and J.-M. Shao, *J. Hazard. Mater.*, 2008, **157**, 201–206.
12 W.-T. Tsai, *J. Fluor. Chem.*, 2007, **128**, 1345–1352.
13 S. Bouvet, B. Pégot, S. Sengmany, E. Le Gall, E. Léonel, A.-M. Goncalves and E. Magnier, *Beilstein J. Org.*

Chem., 2020, **16**, 2948–2953.
14 S. Purser, P. R. Moore, S. Swallow and V. Gouverneur, *Chem. Soc. Rev.*, 2008, **37**, 320–330.
15 M. Inoue, Y. Sumii and N. Shibata, *ACS Omega*, 2020, **5**, 10633–10640.
16 P. Jeschke, *ChemBioChem*, 2004, **5**, 570–589.
17 H. C. Cowen, F. Riding, E. Warhurst, A. D. Buckingham, R. J. W. Le Fèvre, G. D. Meakins, R. N. Haszeldine, J. Jander, G. R. Clemo, B. W. Fox, R. Raper, J. F. W. McOmie, I. M. White, O. L. Brady, P. E. Halstead, A. G. Sharpe, G. W. Gray, B. Jones, J. Cast, T. S. Stevens, F. Bell, J. W. Cook, L. Hunter, R. M. Barrer, N. Mackenzie, D. MacLeod, C. C. Barker, F. D. Casson, G. F. Laws, W. Carruthers, E. S. Lane and C. Williams, *J. Chem. Soc.*, 1953, 4168–4188.
18 C. Berg, T. Braun, M. Ahrens, P. Wittwer and R. Herrmann, *Angew. Chem., Int. Ed.*, 2017, **56**, 4300–4304.
19 G. C. Demitras and A. G. MacDiarmid, *Inorg. Chem.*, 1964, **3**, 1198–1199.
20 H. Deubner and F. Kraus, *Inorganics*, 2017, **5**, 68.
21 P. Holze, B. Horn, C. Limberg, C. Matlachowski and S. Mebs, *Angew. Chem., Int. Ed.*, 2014, **53**, 2750—2753.
22 B. G. Harvey, A. M. Arif, A. Glöckner and R. D. Ernst, *Organometallics*, 2007, **26**, 2872–2879.
23 R. Basta, B. G. Harvey, A. M. Arif and R. D. Ernst, *J. Am. Chem. Soc.*, 2005, **127**, 11924–11925.
24 L. Zámostná, T. Braun and B. Braun, *Angew. Chem., Int. Ed.*, 2014, **53**, 2745–2749.
25 M. Wozniak, T. Braun, M. Ahrens, B. Braun-Cula, P. Wittwer, R. Herrmann and R. Laubenstein, *Organometallics*, 2018, **37**, 821–828.
26 D. Dirican, N. Pfister, M. Wozniak and T. Braun, *Chem. – A Eur. J.*, 2020, **26**, 6945–6963.
27 F. Buß, C. Mück-Lichtenfeld, P. Mehlmann and F. Dielmann, *Angew. Chem., Int. Ed.*, 2018, **57**, 4951–4955.
28 M. Rueping, P. Nikolaienko, Y. Lebedev and A. Adams, *Green Chem.*, 2017, **19**, 2571–2575.
29 T. A. McTeague and T. F. Jamison, *Angew. Chem., Int. Ed.*, 2016, **55**, 15072–15075.
30 P. Tomar, T. Braun and E. Kemnitz, *Chem. Commun.*, 2018, **54**, 9753–9756.
31 P. Tomar, T. Braun and E. Kemnitz, *Eur. J. Inorg. Chem.*, 2019, **2019**, 4735–4739.
32 D. Rombach and H.-A. Wagenknecht, *Angew. Chem., Int. Ed.*, 2020, **59**, 300–303.
33 D. Rombach and H.-A. Wagenknecht, *ChemCatChem*, 2018, **10**, 2955–2961.
34 S. Kim, Y. Khomutnyk, A. Bannykh and P. Nagorny, *Org. Lett.*, 2021, **23**, 190–194.
35 M. R. Crimmin, M. J. Butler and A. J. P. White, *Chem. Commun.*, 2015, **51**, 15994–15996.
36 C. Bakewell, A. J. P. White and M. R. Crimmin, *J. Am. Chem. Soc.*, 2016, **138**, 12763–12766.
37 C. Bakewell, A. J. P. White and M. R. Crimmin, *Angew. Chem., Int. Ed.*, 2018, **57**, 6638–6642.
38 G. Coates, B. J. Ward, C. Bakewell, A. J. P. White and M. R. Crimmin, *Chem. - A Eur. J.*, 2018, **24**, 16282–16286.
39 G. Coates, H. Y. Tan, C. Kalff, A. J. P. White and M. R. Crimmin, *Angew. Chem., Int. Ed.*, 2019, **58**, 12514–12518.
40 G. Coates, F. Rekhroukh and M. R. Crimmin, *Synlett*, 2019, **30**, 2233–2246.
41 N. A. Phillips, G. J. Coates, A. J. P. White and M. R. Crimmin, *Chem. – A Eur. J.*, 2020, **26**, 5365–5368.
42 D. J. Sheldon, G. Coates and M. R. Crimmin, *Chem. Commun.*, 2020, **56**, 12929–12932.
43 V. Jancik, M. M. Moya Cabrera, H. W. Roesky, R. Herbst-Irmer, D. Neculai, A. M. Neculai, M. Noltemeyer and H.-G. Schmidt, *Eur. J. Inorg. Chem.*, 2004, **2004**, 3508–3512.
44 M. P. Mitoraj, A. Michalak and T. Ziegler, *J. Chem. Theory Comput.*, 2009, **5**, 962–975.
45 C. Strohmann, M. Bindl, V. C. Fraaß and J. Hörnig, *Angew. Chem., Int. Ed.*, 2004, **43**, 1011–1014.
46 L. Maron, E. L. Werkema, L. Perrin, O. Eisenstein and R. A. Andersen, *J. Am. Chem. Soc.*, 2005, **127**, 279–292.
47 J. Pinkas and H. W. Roesky, *J. Fluor. Chem.*, 2003, **122**, 125–150.
48 S. Singh and H. W. Roesky, *J. Fluor. Chem.*, 2007, **128**, 369–377.
49 O. Mó, M. Yáñez, M. Eckert-Maksić, Z. B. Maksić, I. Alkorta and J. Elguero, *J. Phys. Chem. A*, 2005, **109**, 4359–4365.
50 K. K. K. Goh, A. Sinha, C. Fraser and R. D. Young, *RSC Adv.*, 2016, **6**, 42708–42712.
51 Y. Ogiwara and N. Sakai, *Angew. Chem., Int. Ed.*, 2020, **59**, 574–594.
52 J. A. Kalow and A. G. Doyle, *J. Am. Chem. Soc.*, 2010, **132**, 3268–3269.
53 Y. Ogiwara, S. Hosaka and N. Sakai, *Organometallics*, 2020, **39**, 856–861.
54 Y. Liang, Z. Zhao, A. Taya and N. Shibata, *Org. Lett.*, 2021, **23**, 847–852.
55 N. J. Sisti, *Encycl. Reagents Org. Synth.*, 2001.
56 B. Fredelake, C. Ebker, U. Klingebiel, M. Noltemeyer and S. Schmatz, *J. Fluor. Chem.*, 2004, **125**, 1007–1017.
57 G. J. Sherborne, A. G. Gevondian, I. Funes-Ardoiz, A. Dahiya, C. Fricke and F. Schoenebeck, *Angew. Chem., Int. Ed.*, 2020, **59**, 15543–15548.

58 J. H. Song, T. Nabeya, Y. Adachi, Y. Ooyama and J. Ohshita, *J. Organomet. Chem.*, 2019, **883**, 47–51.
59 Farnham; William B., US5268511 (A), 1993.
60 R. J. Brotherton, C. J. Weber, C. R. Guibert and J. L. Little, in *Ullmann's Encyclopedia of Industrial Chemistry*, Wiley-VCH, 2000, pp. 237–255, Boron Compounds.
61 H. Heaney, in *Encyclopedia of Reagents for Organic Synthesis*, John Wiley & Sons, Ltd, 2001, Boron Trifluoride.
62 J. A. Gladysz, V. K. Wong and B. S. Jick, *Tetrahedron*, 1979, **35**, 2329–2335.

Supporting information for:

Complete Deconstruction of SF_6 by an Aluminium(I) Compound

Daniel J. Sheldon[a], Mark R. Crimmin*[a]

*Corresponding author. Email: m.crimmin@imperial.ac.uk

[a]Molecular Sciences Research Hub, Department of Chemistry, Imperial College London, 82 Wood Lane, White City, Shepherds Bush, London, W12 0BZ, UK.

Contents

1. General Experimental

Standard Schlenk line and glovebox techniques were used for all manipulations under an inert atmosphere of dinitrogen or argon unless otherwise stated. NMR scale reactions were performed in J. Young NMR tubes equipped with internal standard capillaries of ferrocene (^{1}H NMR spectroscopy) and prepared in a glovebox. An MBraun Labmaster glovebox was utilised, operating at <0.1 ppm H_2O and <0.1 ppm O_2. ^{1}H, ^{13}C, ^{19}F and ^{11}B NMR spectra were recorded on BRUKER 400 MHz or 500 MHz machines, and referenced against $SiMe_4$ (^{1}H, ^{13}C), $CFCl_3$ (^{19}F) and $EtO{\bullet}BF_3$ (^{11}B). Data were processed using the MestReNova software package. Solvents were dried over activated alumina from a solvent purification system (SPS) based upon the Grubbs design and de-gassed before use. Glassware was dried for >6 h prior to use at 120 °C. Benzene-d_6 and toluene-d_8 were de-gassed and stored over 3 Å molecular sieves before use. All reagents were acquired from Sigma Aldrich (Merck), Honeywell or Fluorochem and used without further purification unless specified. Sulfur Hexafluoride was acquired from Apollo Scientific and used without further purification. Where liquids at 25 °C, reagents were dried over activated 3 Å molecular sieves and freeze-pump-thaw degassed prior to use. [{(ArNCMe)$_2$CH}Al] (**1**, Ar = 2,6-di-isopropylphenyl) was prepared following the literature procedure.[1]

2. Synthetic Procedures

2.1 Activation of Sulfur Hexafluoride with [{(ArNCMe)$_2$CH}Al] (1)

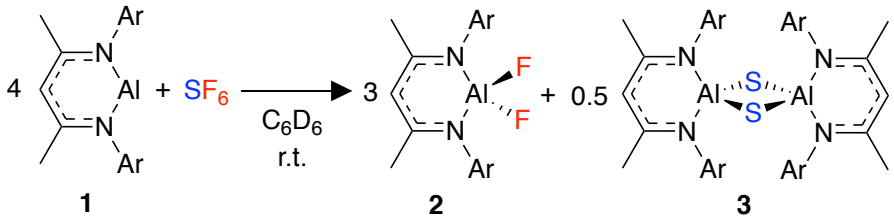

Ar = 2,6-^{i}Pr-C$_6$H$_3$ *67 %* *70 %*

Scheme S1: Activation of SF_6 with **1**.

2.1.1 Isolation of [{(ArNCMe)$_2$CH}AlF$_2$] (2)

In an N_2 filled glovebox, 27 mg (0.06 mmol) of **1** was dissolved in 0.6 mL of C_6D_6, added to a J. Young NMR tube equipped with a ferrocene capillary internal standard, and a t=0 ^{1}H NMR spectrum was recorded. The solution was degassed once *via* freeze-pump-thaw and SF_6 (1 bar, 22 °C) was added. The J. Young tube was inverted multiple times and the red solution turned pale yellow within seconds. The formation of a colourless precipitate was also observed. After 15 minutes, t=1 ^{1}H and ^{19}F NMR spectra were recorded. The 67 % yield of the product [{(ArNCMe)$_2$CH}AlF$_2$] (**2,** Ar = 2,6-di-isopropylphenyl) was determined *in situ* by integral comparison to the ferrocene internal standard in the ^{1}H NMR spectrum. No other species were determined by NMR spectroscopy. The product **2** can be isolated by filtration, removal of C_6D_6 *in vacuo*, and crystallisation from a concentrated *n*-hexane solution.[2]

[{(ArNCMe)$_2$CH}AlF$_2$]: (matching that of literature reports)[2]

^{1}H NMR (400 MHz, C_6D_6, 298 K): δ 1.10 (d, 12H, CH(C$\underline{H}_3$)$_2$, $^3J_{HH}$ = 6.8 Hz), 1.42 (d, 12H, CH(C$\underline{H}_3$)$_2$, $^3J_{HH}$ = 6.8 Hz), 1.53 (s, 6H, C$\underline{H}_3$), 3.31 (sept, 4H, C$\underline{H}$(CH$_3$)$_2$, $^3J_{HH}$ = 6.8 Hz), 4.94 (s, 1H, C(CH$_3$)C$\underline{H}$C(CH$_3$)), 7.05-7.15 (m, 6H, Ar$\underline{H}$); ^{19}F NMR (376.5 MHz, C_6D_6, 298 K): δ -173.6 (2F, Al$\underline{F}$)

SF_6:

^{19}F NMR (376.5 MHz, C_6D_6, 298 K): δ 58.4 (6F)

2.1.2 Isolation of [{(ArNCMe)$_2$CH}Al(μ-S)]$_2$ (3)

The reaction was carried out in the same manner but with no agitation of the NMR tube after addition of the gas, allowing for slow diffusion of SF_6 into the C_6D_6 solution of **1**. Single-crystals

of the insoluble product **3** grew over a period of 2 days, in a 70 % isolated yield. These crystals were suitable for single-crystal x-ray diffraction, allowing the confirmation of the structure of **3**. It is noted that **3** was found to be insoluble in all common laboratory solvents, consistent with the findings of the original literature report.[3]

IR Data: (matching very closely to that of the literature report)[3]

v(cm^{-1}): 3056 (vw), 2956 (m), 2924 (str), 2849 (m), 1587 (vw), 1531 (str), 1461 (m), 1436 (m), 1382 (str), 1316 (str), 1291 (vw, shoulder of peak), 1249 (m), 1174 (w), 1103 (vw), 1056 (vw), 1021 (w), 936 (vw), 867 (w), 804 (w), 775 (w), 763 (w)

X-ray Crystal Structure of 3

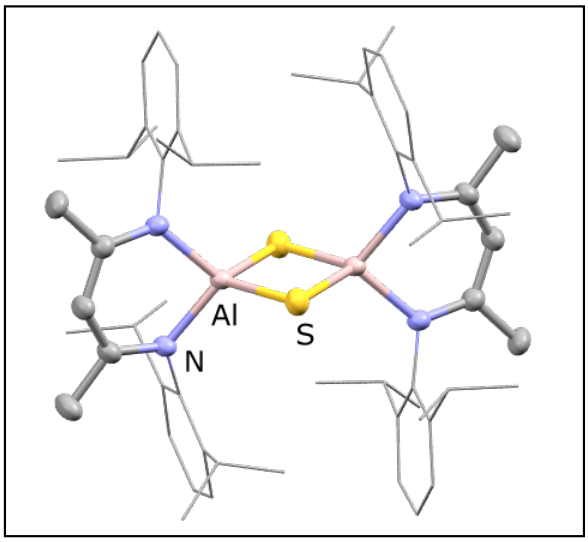

Figure S1: X-ray crystal structure of **3**. Hydrogen atoms omitted for clarity.

*Crystal Data for **3*** ($C_{58}H_{82}Al_2N_4S_2$), M =953.35, monoclinic, space group C2/c (no. 15), a = 22.3453(5) Å, b = 14.7350(3) Å, c = 16.3947(3) Å, β = 90.3187(18)°, V = 5398.01(18) $Å^3$, Z = 4, $\rho_{calc}g/cm^3$ = 1.173, μ(Cu Kα) = 1.507 mm^{-1}, T = 173.10(14), clear light colourless blocks, F^2 refinement, R_1(obs) = 0.0564, wR_2(all) = 0.1734, 5181 independent observed reflections (R_{int} = 0.0285), 4243 independent measured reflections [$|F_o| > 4\sigma(|F_o|)$, $2\theta_{full}$ = 146.876], 308 parameters. CCDC deposition number: 2084888. Data were collected using Agilent Xcalibur PX Ultra A diffractometer.

3 was found to crystallise in the space group (C2/c). There was no solvent or disorder to be modelled. The structure we report is a different polymorph to that previously reported in the literature, which crystallised in the space group C2/m, although both are monoclinic.[3] The

bonding metrics are found to be almost identical (Table S1), crucially both suggesting an almost planar and symmetrical Al_2S_2 ring.

	Literature Report (see reference 3)	Crystal Data Reported Here
Al-N	1.928(2)	1.944(2)/1.939(2)
Al-S	2.237(1)	2.2136(9)
Al-S1	2.245(1)	2.2171(9)
S-Al-S	96.5(1)	97.52(3)
Al-S-Al	83.5(1)	82.48(3)
N-Al-N	94.9(1)	93.92(9)

Table S1: Comparison of bond metrics to literature report.

2.2 Reactivity of [{(ArNCMe)$_2$CH}AlF$_2$] (2)

2.2.1 Reactivity of [{(ArNCMe)$_2$CH}AlF$_2$] (2) with a Silicon Electrophiles

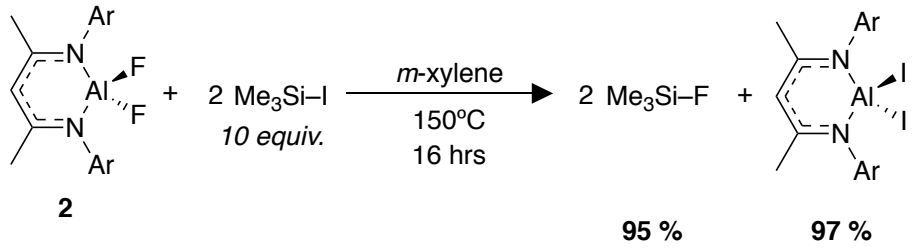

2

95 % **97 %**

Scheme S2: Conditions for reaction of **2** with a silicon electrophile

In an N_2 filled glovebox, 51.8 µL of a 0.2 M stock solution (0.010 mmol) of **2** in *m*-xylene was added to a J Young NMR tube along with a further 530 µL of *m*-xylene, 20 µL of a 0.1 M stock solution of 1,2-difluorobenzene (internal standard) in C_6D_6, and 0.10 mmol (10 equiv.) of the relevant electrophile. The J Young NMR tube was equipped with a capillary internal standard containing ferrocene in C_6D_6, and t=0 ^{1}H and ^{19}F NMR spectra were recorded. The NMR tube was then placed in a 150°C oil bath for a set amount of time, before further ^{1}H and ^{19}F spectra were recorded. Quantitative ^{19}F integration was performed using the 1,2-difluorobenzene triplet at δ -138.0 ppm, while quantitative ^{1}H integration was performed using the ferrocene singlet at δ 4.0 ppm, or through external addition of 1,3,5-trimethoxybenzene and comparison of singlet at δ 6.33 in *m*-xylene (this peak comes at δ 6.26 in C_6D_6).

NMR Characterisation of Products:

Fluorotrimethylsilane: (in very close agreement with literature reports)[4]

^{19}F NMR (C_6D_6, 100 MHz, 298K): -157.2 (sept, $^3J_{HH}$ = 7.0 Hz).

^{1}H NMR (*m*-xylene, C_6D_6 insert, 400 MHz): 0.11 (d, $^3J_{HH}$ = 7.0 Hz).

[{(ArNCMe)$_2$CH}AlI$_2$]: (in very close agreement with literature reports)[1]

^{1}H NMR (C_6D_6, 400 MHz, 298 K): 7.1-7.2 (m, 6 H, Ph), 5.05 (s, 1 H, *γ*–C<u>H</u>), 3.59 (sept, 4 H, $^3J_{HH}$ = 6.8 Hz, C<u>H</u>Me$_2$), 1.49 (s, 6 H, Me), 1.43 (d, 12 H, $^3J_{HH}$ = 6.80 Hz, CH<u>Me$_2$</u>), 1.08 (d, 12 H, $^3J_{HH}$ = 6.8 Hz, CH<u>Me$_2$</u>).The formation of this compound was confirmed by independent synthesis.

2.2.2 Reactivity of [{(ArNCMe)$_2$CH}AlF$_2$] (2) with Boron Electrophiles

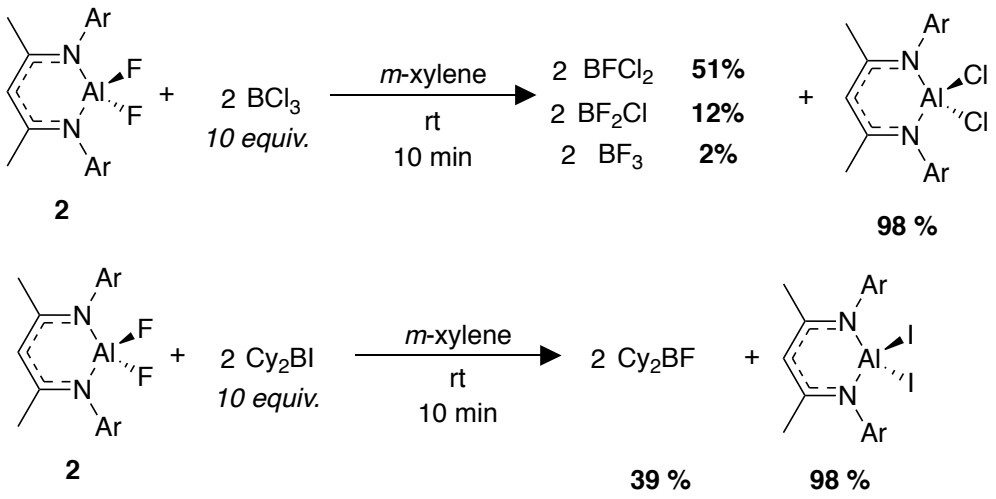

Scheme S3: Conditions for reaction of **2** with boron electrophiles

In an N_2 filled glovebox, 51.8 µL of a 0.2 M stock solution (0.010 mmol) of **2** in *m*-xylene was added to a J Young NMR tube along with a further 530 µL of *m*-xylene, 20 µL of a 0.1 M stock solution of 1,2-difluorobenzene in C_6D_6, and the J Young NMR tube was equipped with a capillary internal standard containing ferrocene in C_6D_6. Then, on the Schlenk line, 0.10 mmol (10 equiv.) of the relevant boron electrophile was added under a N_2 atmosphere. ^{1}H, ^{19}F and ^{11}B NMR spectra were recorded. Quantitative ^{19}F integration was performed using the 1,2-difluorobenzene triplet at δ -138.0 ppm, while quantitative ^{1}H integration was performed using the ferrocene singlet at δ 4.0 ppm, or through external addition of 1,3,5-trimethoxybenzene and comparison of singlet at δ 6.33 in *m*-xylene (peak comes at δ 6.26 in C_6D_6).

NMR Characterisation of Products:

[{(ArNCMe)$_2$CH}AlI$_2$]: (in very close agreement with literature reports)[1]

^{1}H NMR (C_6D_6, 400 MHz, 298 K): 7.1-7.2 (m, 6 H, Ph), 5.05 (s, 1 H, *γ*–C<u>H</u>), 3.59 (sept, 4 H, $^3J_{HH}$ = 6.8 Hz, C<u>H</u>Me$_2$), 1.49 (s, 6 H, Me), 1.43 (d, 12 H, $^3J_{HH}$ = 6.80 Hz, CH<u>Me$_2$</u>), 1.08 (d, 12 H, $^3J_{HH}$ = 6.8 Hz, CH<u>Me$_2$</u>). The formation of this compound was confirmed by independent synthesis.

[{(ArNCMe)$_2$CH}AlCl$_2$]: (in very close agreement with literature reports)[5]

^{1}H NMR (C_6D_6, 400 MHz, 298 K): 7.1-7.2 (m, 6 H, Ph), 4.91 (s, 1 H, *γ*–C<u>H</u>), 3.44 (sept, 4 H, $^3J_{HH}$ = 6.8 Hz, C<u>H</u>Me$_2$), 1.50 (s, 6 H, Me), 1.42 (d, 12 H, $^3J_{HH}$ = 6.80 Hz, CH<u>Me$_2$</u>), 1.10 (d, 12 H, $^3J_{HH}$ = 6.8 Hz, CH<u>Me$_2$</u>).

BCl$_2$F: (in very close agreement with literature reports)[6]

^{19}F NMR (*m*-xylene, C_6D_6 insert, 100 MHz, 298 K): -27.7, 1:1:1:1 quartet, $^1J_{BF}$ = 72 Hz)

^{11}B NMR (*m*-xylene, C_6D_6 insert, 128 MHz, 298 K): 32.6, d, $^1J_{BF}$ = 74 Hz)

$BClF_2$: (in very close agreement with literature reports)[6]

^{19}F NMR (*m*-xylene, C_6D_6 insert, 100 MHz, 298 K): -74.4, 1:1:1:1 quartet (coupling poorly resolved), $^1J_{BF}$ = 35 Hz)

^{11}B NMR (*m*-xylene, C_6D_6 insert, 128 MHz, 298 K): 20.0, tr, $^1J_{BF}$ = 33 Hz)

BF_3: (in very close agreement with literature reports)[6]

^{19}F NMR (*m*-xylene, C_6D_6 insert, 100 MHz, 298 K): -125.8, 1:1:1:1 quartet (coupling poorly resolved), $^1J_{BF}$ = 10 Hz)

^{11}B NMR (*m*-xylene, C_6D_6 insert, 128 MHz, 298 K): 9.9, q, coupling unresolved)

Cy_2BF:

^{19}F NMR (C_6D_6, 100 MHz, 298 K): -42.2, m (br)

^{11}B NMR (C_6D_6, 128 MHz, 298 K): 58.2, m (br)

^1H NMR (C_6D_6, 400 MHz, 298 K): 0.88 – 1.88, m, cyclohexyl). *^1H spectrum was contaminated with a very minor amount of* ***[{(ArNCMe)$_2$CH}AlI$_2$].***

2.2.3 Reactivity of [{(ArNCMe)$_2$CH}AlF$_2$] (2) with Carbon Electrophiles

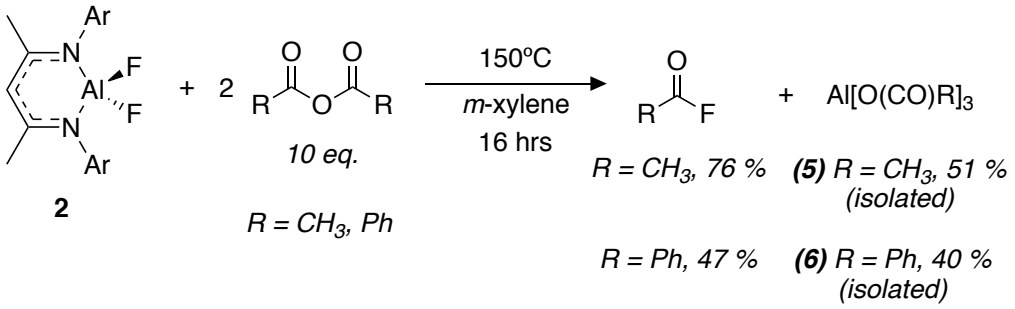

Scheme S4: Conditions for reaction of **2** with carbon electrophiles

NMR Procedure: In an N_2 filled glovebox, 51.8 µL of a 0.2 M stock solution (0.010 mmol) of **2** in *m*-xylene was added to a J Young NMR tube along with a further 530 µL of *m*-xylene, 20 µL of a 0.1 M stock solution of 1,2-difluorobenzene (internal standard) in C_6D_6 and 0.10 mmol (10 equiv.) of the relevant electrophile. The J Young NMR tube was equipped with a capillary internal standard containing ferrocene in C_6D_6, and t=0 ^{1}H and ^{19}F NMR spectra were recorded. The NMR tube was then placed in a 150°C oil bath for a set amount of time, before further ^{1}H and ^{19}F spectra were recorded. Quantitative ^{19}F integration was performed using the 1,2-difluorobenzene triplet at δ -138.0 ppm, while quantitative ^{1}H integration was performed using the ferrocene singlet at δ 4.0 ppm, or through external addition of 1,3,5-trimethoxybenzene and comparison of singlet at δ 6.33 in *m*-xylene (this peak comes at δ 6.26 in C_6D_6). It was noted that a colourless precipitate also formed in the NMR tube, which was found to be insoluble in NMR solvents (see below for preparative procedure).

NMR Characterisation of Products:

Benzoyl Fluoride: (in very close agreement with literature reports)[7]

^{1}H NMR (C_6D_6, 400 MHz, 298 K): 7.67 (d, 2H, $^3J_{HH}$ = 7.7 Hz, o-CH), 6.99 (t, 1H, $^3J_{HH}$ = 7.5 Hz, p-CH), 6.82 (t, 2H, $^3J_{HH}$ = 8.6 Hz, m-CH). ^{19}F NMR (C_6D_6, 100 MHz, 298 K): 18.0 (s).

Acetyl Fluoride: (in very close agreement with literature reports)[7]

^{19}F NMR (C_6D_6, 100 MHz, 298 K): 50.6 (s).

Preparative Procedure:

Reaction with Acetic Anhydride:

In an N_2 filled glovebox, 200 mg (0.41 mmol) of **2** was added to a J Young ampoule equipped with a stirrer bar, along with 423 mg (4.1 mmol, 10 equivs.) of acetic anhydride, and 5 mL of *m*-xylene. The reaction mixture was stirred and heated to 150°C in a silicon oil bath overnight. A colourless precipitate was observed to form, as observed on the NMR scale. The mixture was left to settle, before the solid precipitate was isolated by filtration of the liquid fraction, washed with n-hexane (3 x 5 mL) and toluene (3 x 5 mL), and dried *in vacuo* for 6 hours (43 mg, 0.21 mmol, 51 %). This compound (Scheme S4, compound **5**), was found to be insoluble in NMR solvents, and thus was subjected to IR spectroscopy for analysis (see below).

Reaction with Benzoic Anhydride:

In an N_2 filled glovebox, 200 mg (0.41 mmol) of **2** was added to a J Young ampoule equipped with a stirrer bar, along with 937 mg (4.1 mmol, 10 equivs.) of benzoic anhydride, and 5 mL of *m*-xylene. The reaction mixture was stirred and heated to 150°C in a silicon oil bath overnight. A colourless precipitate was observed to form, as observed on the NMR scale. The mixture was left to settle, before the solid precipitate was isolated by filtration of the liquid fraction, washed with n-hexane (3 x 5 mL) and toluene (3 x 5 mL), and dried *in vacuo* for 6 hours (66 mg, 0.17 mmol, 40 %). This compound (Scheme S4, compound **6**), was found to be insoluble in NMR solvents, and thus was subjected to IR spectroscopy for analysis (see below).

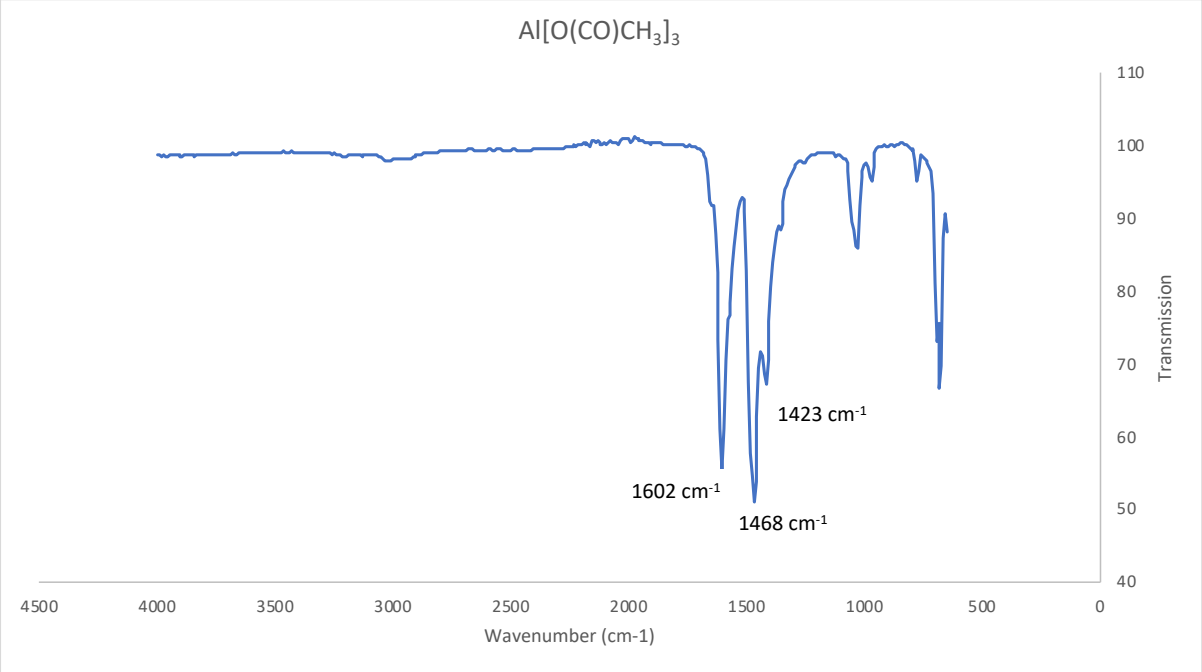

Figure S2: IR spectrum of $Al[O(CO)CH_3]_3$, **5**

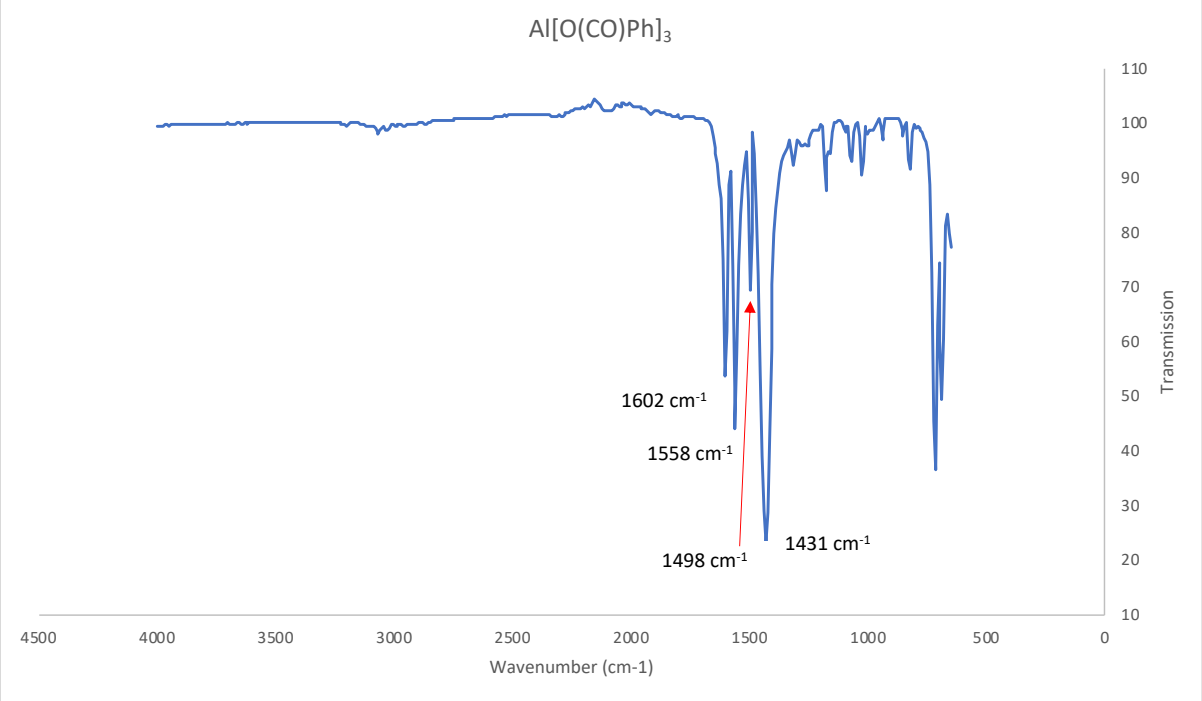

Figure S3: IR spectrum of $Al[O(CO)Ph]_3$, **6**

Compound **5** and **6** show a similar pattern (compound 6 data in parenthesis): a strong peak at 1602 cm^{-1} (1602 cm^{-1}) and 1468 cm^{-1} (1558 cm^{-1}), and then a weaker peak at 1423 cm^{-1} (1498 cm^{-1}). These stretches fall in the typical region for asymmetric and symmetric COO^- stretches, based on similar stretches observed for other metal carboxylates in the literature.[8,9] We propose the products are tris-carboxylates of the form $Al(O(CO)CH_3)_3$ **(5)** and $Al(O(CO)Ph)_3$

(6). Although it is difficult to say with certainty whether the bonding mode is unidentate or bidentate, previous work suggests that presence of a symmetric COO^- stretch indicates a bidentate bonding mode.[9] The proposed compound **5** has some precedence in the literature, albeit with very limited data.[10,11] It was found to be insoluble in benzene and dioxane. It was characterised only by CHN analysis. A similar lack of experimental data was found for **6** or similar compounds.

In order to further this identification, independent syntheses of the aluminium products were carried out (Scheme S5).

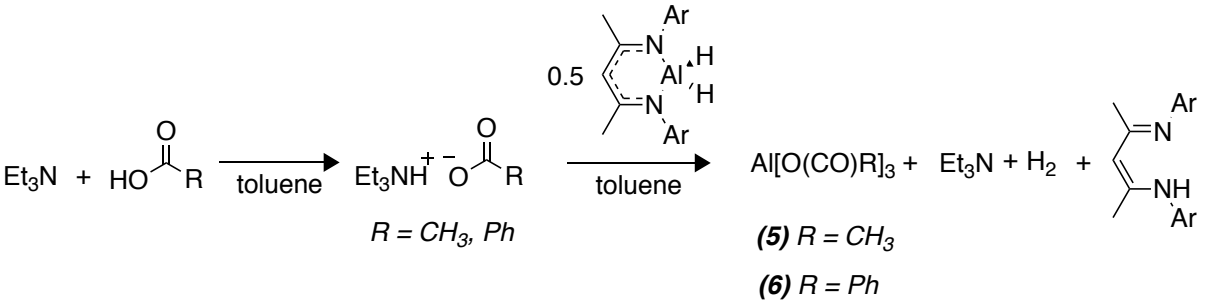

Scheme S5: Independent syntheses of aluminum by-products

Independent Synthesis of Al-containing Side product 5: Triethylamine (172 mg, 1.7 mmol) and acetic acid (102 mg, 1.7 mmol) were stirred in a toluene solution (3 mL) for 1 hour. The solvent was removed *in vacuo*. The residue was redissolved in toluene (3 mL) and 0.5 equiv of [{(ArNCMe)$_2$CH}AlH$_2$] (380 mg, 0.85 mmol) (synthesised as per ref. 12) was added.[12] Immediately a colourless precipitate formed. The reaction was stirred for 30 minutes. The solid precipitate was isolated by decanting the liquid fraction, before washing with hexane (3 x 1 mL). The solid was investigated by IR spectroscopy (see below), which was found to be in close agreement with the IR data above, and thus also assigned as compounds **5**. ^{1}H NMR spectroscopy of the liquid fraction from this reaction revealed the parent, protonated, β-diketiminate ligand.[13]

Independent Synthesis of Al-containing Side product 6: Triethylamine (172 mg, 1.7 mmol) and benzoic acid (207 mg, 1.7 mmol) were stirred in a toluene solution (3 mL) for 1 hour. The solvent was removed *in vacuo*. The residue was redissolved in toluene (3 mL) and 0.5 equiv of [{(ArNCMe)$_2$CH}AlH$_2$] (380 mg, 0.85 mmol) (synthesised as per ref. 12) was added.[12] Immediately a colouress precipitate formed and the reaction was stirred for 30 minutes. The solid precipitate was isolated by decanting the liquid fraction, before washing with hexane (3 x 1 mL). The solid was investigated by IR spectroscopy (see below), which was found to be in close agreement with the IR data above, and thus also assigned as compounds **6.** ^{1}H NMR spectroscopy of the liquid fraction from this reaction revealed the parent, protonated, β-diketiminate ligand.[13]

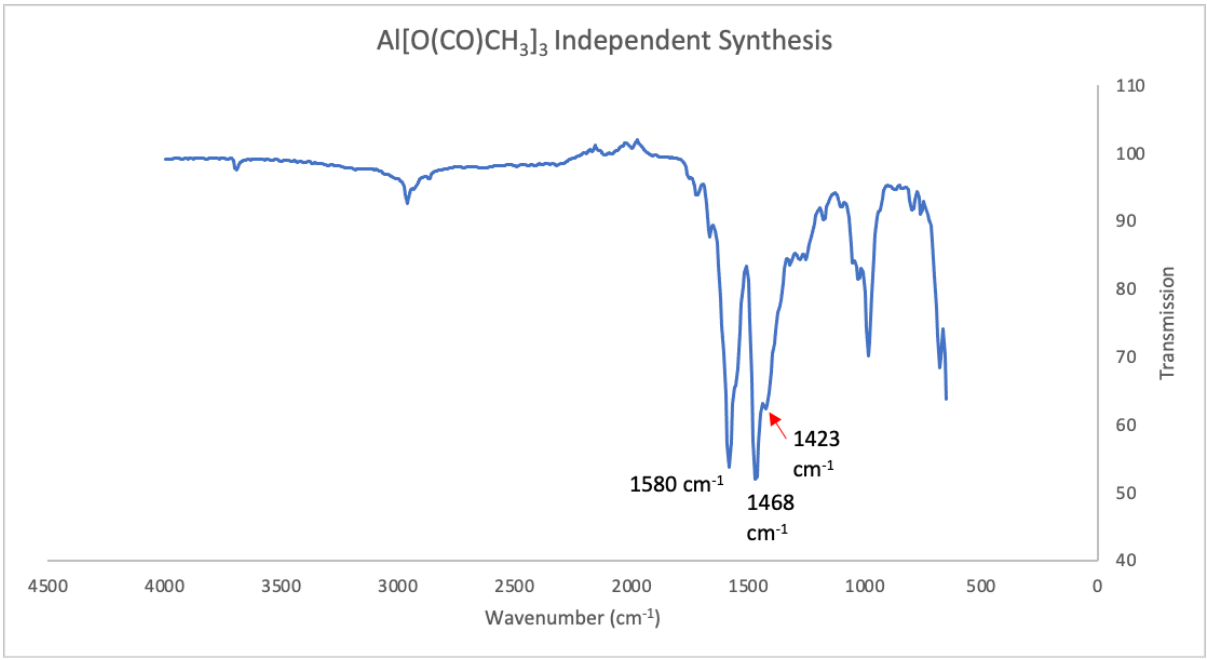

Figure S4: IR spectrum of independently synthesised Al[O(CO)CH_3]$_3$, **5**

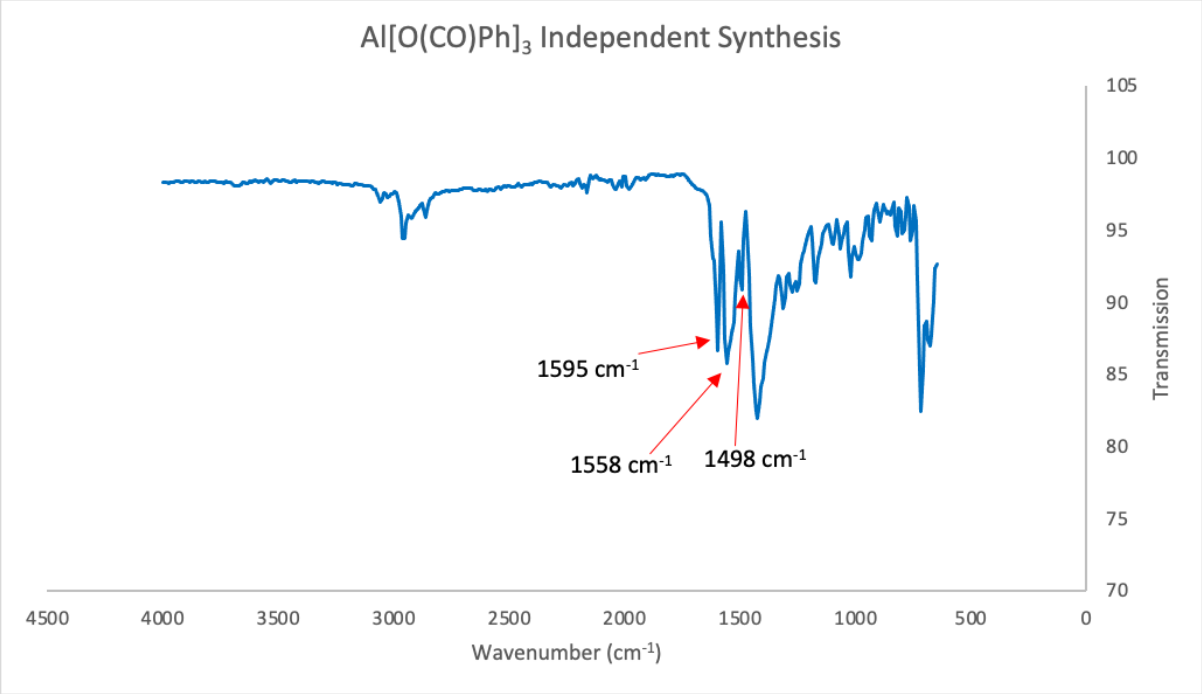

Figure S5: IR spectrum of independently synthesised Al[O(CO)Ph]$_3$, **6**

2.3 Reactivity of [{(ArNCMe)$_2$CH}Al(μ-S)]$_2$ (3)

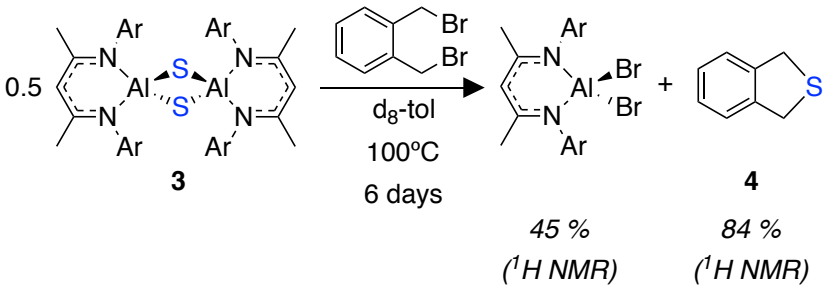

Scheme S6: Reaction conditions for the sulfide transfer from **3** to form heterocycle **4**.

Reaction of 3 with α,α′-dibromo-o-xylene: 10 mg (0.01 mmol) of **3** was added to a J Young NMR tube, along with 27.7 mg (0.10 mmol) of α,α′-dibromo-*o*-xylene, and 0.6 mL toluene-d$_8$. The J Young NMR tube was placed in a silicon oil bath at 100°C for 6 days. ^{1}H NMR spectroscopy revealed the formation of [{(ArNCMe)$_2$CH}AlBr$_2$] in a 45 % yield,[14] and the sulfur heterocycle 1,3-dihydrobenzothiophene in an 84 % yield.[15,16] Yields were determined by integral comparison to 1,3,5-trimethoxybenzene internal standard (6.16, s, 3H, C<u>H</u>).

[{(ArNCMe)$_2$CH}AlBr$_2$]: (in very close agreement with literature reports)[14]
^{1}H NMR (toluene-d$_8$, 400 MHz, 298 K): 7.01-7.15 (m, 6 H, Ph), 4.93 (s, 1 H, γ–C<u>H</u>), 3.46 (sept, 4 H, $^3J_{HH}$ = 6.8 Hz, C<u>H</u>Me$_2$), 1.50 (s, 6 H, Me), 1.40 (d, 12 H, $^3J_{HH}$ = 6.80 Hz, CH<u>Me$_2$</u>), 1.10 (d, 12 H, $^3J_{HH}$ = 6.8 Hz, CH<u>Me$_2$</u>).

1,3-dihydrobenzothiophene: (in very close agreement with literature reports)[16]
^{1}H NMR (CDCl$_3$, 400 MHz, 298 K): 7.27-7.14 (m, Ar, 4H), 4.28 (s, C<u>H$_2$</u>, 4H). *^{1}H NMR spectrum also contained some of the excess starting material α,α′-dibromo-o-xylene: 7.40-7.36 (m, 2H), 7.34-7.30 (m, 2H), 4.68 (s, 4H).*

3. Computational Methods

DFT calculations were run using Gaussian 09 (Revision D.01)[17] using the M06-2X Minnesota functional and an ultrafine integration grid (keyword int=ultrafine).[18] Al centres were described with Stuttgart SDDAll RECPs and associated basis sets, while a hybrid basis set was used for the other atoms: 6-31g**(C, H)/6-311+g*(S, N, F).

Geometry optimisation calculations were performed without symmetry constraints. The Gaussian 09 default optimisation criteria were tightened to 10^{-9} on the density matrix and 10^{-7} on the energy matrix. The default numerical integration grid was also improved using a pruned grid with 99 radial shells and 590 angular points per shell. Frequency analyses for all stationary points were performed using the enhanced criteria to confirm the nature of the structures as either minima (no imaginary frequency) or transition states (only one imaginary frequency). Single point solvent corrections (benzene, $\varepsilon = 2.2706$) were applied using the polarizable continuum model (PCM) to free energies.[19] Single point dispersion corrections using Grimme's D3 correction were applied to free energies.[20] Intrinsic reaction coordinate (IRC) calculations followed by full geometry optimisations on final points were used to connect transition states and minima located on the potential energy surface allowing a full energy profile (calculated at 298.15 K, 1 atm) of the reaction to be constructed.[21,22] The graphical user interface used to visualise the various properties of the intermediates and transition states was GaussView 5.0.9.[23] Natural Bond Orbital analysis was carried out using NBO 6.0.[24]

ETS-NOCV[25] calculations were performed using DFT as implemented in Orca 4.2.1.[26,27] Optimised geometries from the Gaussian 09 calculations detailed above were used. Single-point calculations were performed using the M06-2X functional[18] with Grimme's D3 dispersion correction[20] applied, and an ultrafine (99,950) grid (grid6). The def2-tzvpp basis set was used for all atoms.

3.1 NBO Data and Analysis

A full NBO analysis was carried out and the relevant NPA charges and Wiberg Bond Indices are tabulated below.

It is noted in the manuscript that for **TS-1** and **TS-2**, the second S–F cleavage occurs after the transition state has been surmounted. An IRC calculation connects **TS-1** directly to SF_4 and [{(ArNCMe)$_2$CH}AlF_2], suggesting a barrierless process for the second bond cleavage. Likewise for **TS-2**, an IRC calculation connects **TS-2** directly to SF_2 and [{(ArNCMe)$_2$CH}AlF_2].

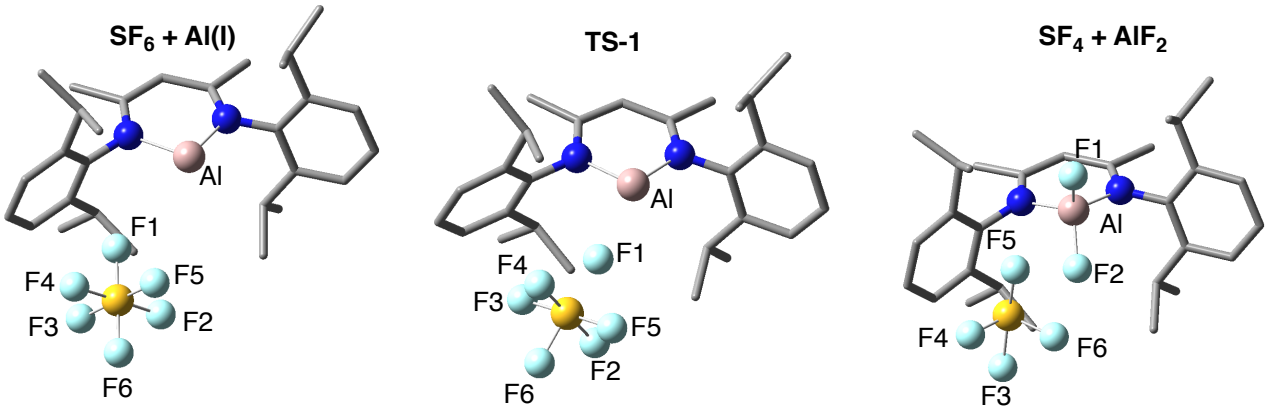

NPA Charge	SF_6 + Al(I)	TS-1	Al-F_2 + SF_4
S	+2.61	+2.46	+2.00
F1	-0.41	-0.51	-0.81
F2	-0.43	-0.47	-0.82
Al	+0.83	+1.13	+2.30

Table S2: NPA charges for TS-1

WBI	SF_6 + Al(I)	TS-1	Al-F_2 + SF_4
S–F1	0.71	0.49	0.00
S–F2	0.69	0.63	0.02
S–F3	0.70	0.64	0.60
S–F4	0.69	0.64	0.76
S–F5	0.69	0.64	0.62
S–F6	0.69	0.69	0.78
Al–F1	0.02	0.16	0.32
Al–F2	0.00	0.04	0.28

Table S3: WBI indices for TS-1

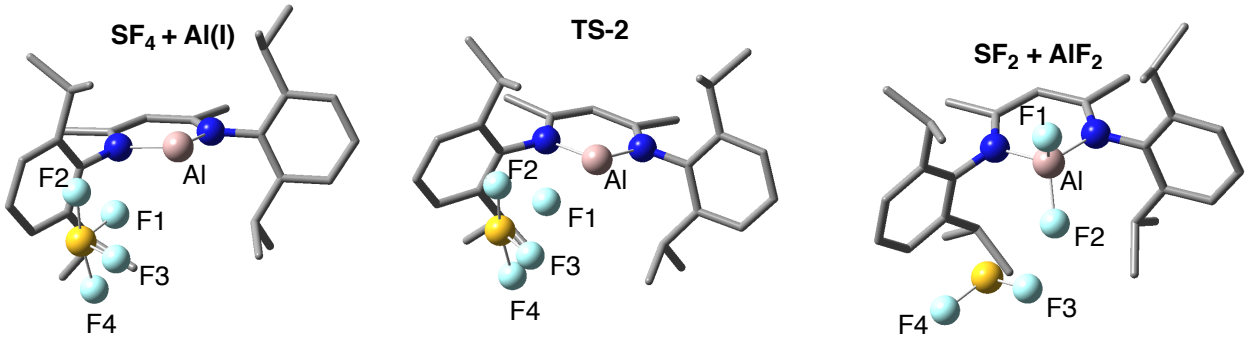

NPA Charge	Al(I) + SF_4	TS-2	Al-F_2 + SF_2
S	1.95	1.75	0.97
F1	-0.41	-0.53	-0.81
F2	-0.55	-0.56	-0.81
F3	-0.44	-0.44	-0.47
F4	-0.56	-0.57	-0.49
Al	0.84	1.15	2.30

Table S4: NPA charges for TS-2

Wiberg Bond Index	Al(I) + SF_4	TS-2	Al-F_2 + SF_2
S–F1	0.79	0.50	0.001
S–F2	0.63	0.60	0.03
S–F3	0.77	0.76	0.79
S–F4	0.61	0.59	0.76
Al–F1	0.02	0.19	0.32
Al–F2	0.001	0.001	0.28

Table S5: WBI Indices for TS-2

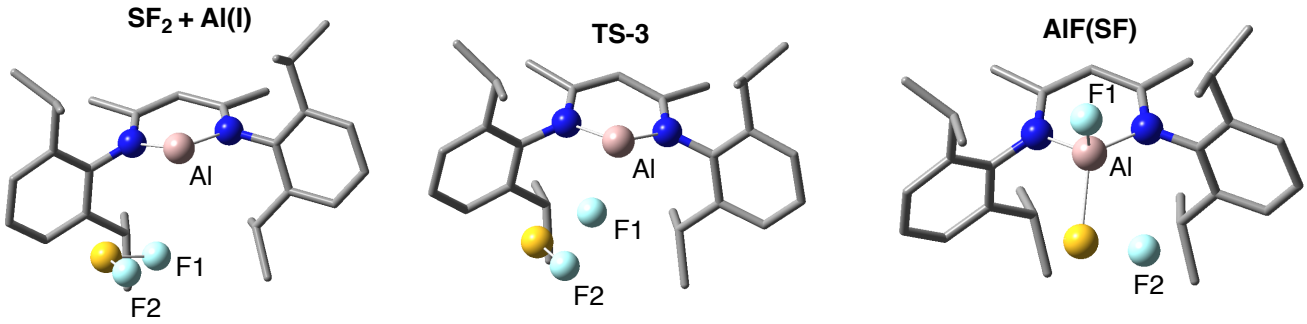

NPA charge	Al(I) + SF_2	TS-3	Al(F)(SF)
S	0.95	0.78	-0.04
F1	-0.47	-0.60	-0.80
F2	-0.46	-0.47	-0.48
Al	0.83	1.08	2.00

Table S6: NPA charges for TS-3

WBI	Al(I) + SF_2	TS-3	Al(F)(SF)
S–F1	0.76	0.48	0.02
S–F2	0.79	0.78	0.75
Al-F1	0.03	0.17	0.33
Al-F2	0.01	0.02	0.03
Al-S	0.06	0.39	0.67

Table S7: WBI Indices for TS-3

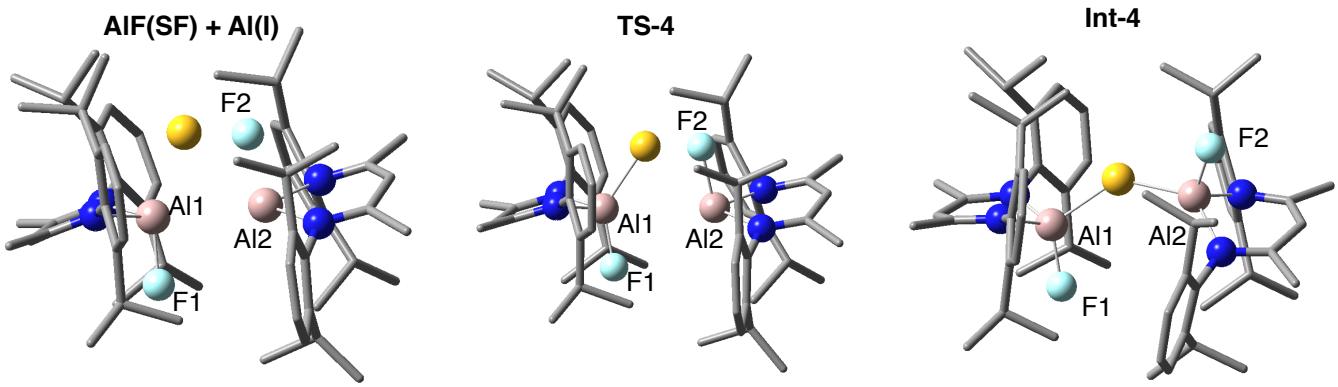

NPA charge	Al(l) + Al-(F)(SF)	TS-4	Int-4
S	-0.08	-0.23	-1.21
F1	-0.84	-0.83	-0.82
F2	-0.59	-0.66	-0.81
Al1	1.57	1.81	2.10
Al2	1.41	1.41	2.08

Table S8: NPA charges for TS-4

WBI	Al(l) + Al-(F)(SF)	TS-4	Int-4
Al1-S	0.46	0.63	0.61
Al1-F1	0.24	0.26	0.31
S-F2	0.56	0.43	0.02
Al2-F2	0.11	0.18	0.31
Al2-S	0.15	0.35	0.64

Table S9: WBI Indices for TS-4

NPA charge	SF_6	SF_4	SF_2
S	2.61	1.93	0.91
F	-0.43	-0.54 (axial)	-0.46
F	-0.43	-0.54 (axial)	-0.46
F	-0.43	-0.42 (equatorial)	
F	-0.43	-0.42 (equatorial)	
F	-0.43		
F	-0.43		

Table S10: NPA charges for SF_6, SF_4 and SF_2

WBI	SF_6	SF_4	SF_2
S–F	0.70	0.64 (axial)	0.81
S–F	0.70	0.64 (axial)	0.81
S–F	0.70	0.79 (eq.)	
S–F	0.70	0.79 (eq.)	
S–F	0.70		
S–F	0.70		

Table S11: WBI Indices for SF_6, SF_4 and SF_2

3.2 ETS-NOCV

ETS-NOCV calculations were carried out on **TS-1**, **TS-2** and **TS-3** (Table S12). They suggest that the major contribution ($\Delta\rho_1$) to the orbital interaction energy of the two fragments (**1** and SF_x (x=6,4,2) is from the Al lone pair to the σ* S–F orbital. The interpretation of this data is taken with caution due to the limitations of using DFT generated orbitals to depict the electronic structure of transition states. However, the calculations still suggest a qualitative understanding of the flow of electron density.

Transition-State ΔE_{orb}	$\Delta\rho_1$
TS-1 ***-21 kcal mol^{-1}***	$\Delta\rho_1$ Al(3s) to σ*S–F -17 kcal mol^{-1} 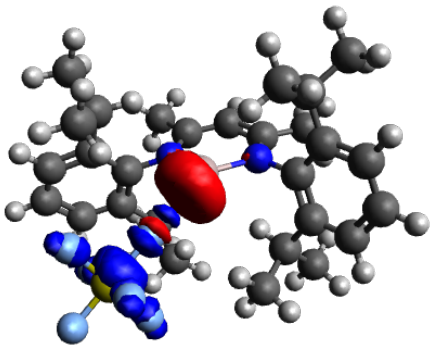
TS-2 **-25 kcal mol^{-1}**	$\Delta\rho_1$ Al(3s) to σ*S–F - 18 kcal mol^{-1} 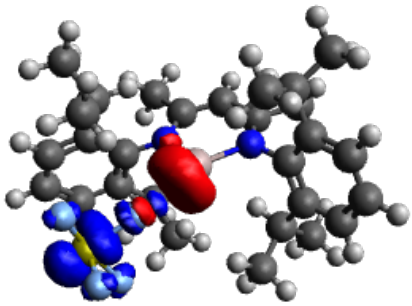
TS-3 **-37 kcal mol^{-1}**	$\Delta\rho_1$ Al(3s) to σ*S–F - 22 kcal mol^{-1} 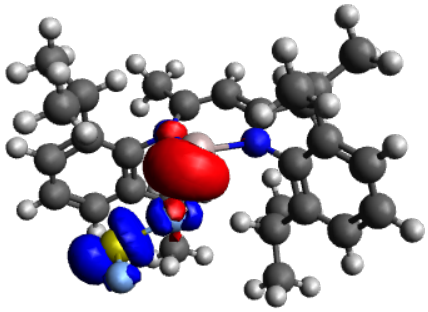

Table S12: Selected deformation density data on transition states **TS-1**, **TS-2**, **TS-3**. Charge flow from red to blue.

3.3 Functional Benchmarking

An assessment of the computational methodology was carried out by a series of functional benchmarking calculations (Table S13). The functionals tested were the Minnesota hybrid-meta functional M06-2X,[18] the long-range corrected functional ω-B97X,[28] and with Grimme's D2 dispersion correction ω-B97X-D.[29] The same basis set and pseudopotential combination were maintained throughout. Single point solvent corrections (benzene, ε = 2.2706) were applied using the polarizable continuum model (PCM) to free energies.[19] Single point

dispersion corrections using Grimme's D3 correction were applied to free energies in the cases of M06-2X and ω-B97X (noting that ω-B97X-D has Grimme's D2 dispersion correction built into the functional).[20] Consistent results were found across the different functionals (Table S13).

	M06-2X	ω-B97X	ω-B97X-D
$\Delta G_{TS\text{-}1}^{\ddagger}$	10	9	10
$\Delta G_{TS\text{-}2}^{\ddagger}$	11	13	14
$\Delta G_{TS\text{-}3}^{\ddagger}$	11	15	15
$\Delta G_{TS\text{-}4}^{\ddagger}$	3	8	7

Table S13: Relative free-energy barriers for the four transition states calculated for various density functionals. Free-energies in kcal mol^{-1}.

3.4 XYZ Coordinates

1.log

SCF (M062X) = -1240.85289427

E(SCF)+ZPE(0 K)= -1240.209482

H(298 K)= -1240.173426

G(298 K)= -1240.275279

Lowest Frequency = 20.8423cm-1

Al	10.188542	1.553179	3.544343
N	9.056951	2.897809	4.542831
N	10.522811	2.991042	2.162315
C	8.945094	4.209605	4.348456
C	9.519203	4.877777	3.260244
H	9.357249	5.945679	3.201947
C	10.211486	4.283235	2.196774
C	8.128099	5.034415	5.315415
H	7.069061	4.765572	5.242332
H	8.235270	6.098778	5.107843
H	8.434032	4.831717	6.345193
C	10.611746	5.175546	1.045003

H	10.234433	4.772050	0.101297
H	11.701789	5.216367	0.955804
H	10.230096	6.186713	1.182798
C	8.292211	2.296262	5.598995
C	6.945880	1.957301	5.351260
C	6.230752	1.303923	6.354027
H	5.194582	1.030347	6.180311
C	6.824651	0.991522	7.572245
H	6.253647	0.479588	8.340124
C	8.148220	1.336505	7.801424
H	8.609363	1.092473	8.754719
C	8.905528	1.992207	6.826316
C	6.293304	2.251468	4.008091
H	6.846558	3.065703	3.528522
C	6.395111	1.027017	3.089380
H	7.436341	0.712383	2.955962
H	5.971879	1.246849	2.103061
H	5.848655	0.181181	3.519692
C	4.835770	2.703616	4.137949
H	4.732474	3.530444	4.847074
H	4.187857	1.888639	4.474634
H	4.459617	3.035124	3.165994
C	10.349310	2.359015	7.128519
H	10.754340	2.884352	6.257149
C	10.445081	3.306625	8.330882
H	9.853013	4.213657	8.178439
H	11.484739	3.601621	8.500898
H	10.082897	2.821617	9.242982
C	11.200993	1.105354	7.361993
H	11.157224	0.436035	6.498323
H	10.848454	0.553305	8.239576

H	12.245726	1.380760	7.536358
C	11.178040	2.473376	0.994208
C	12.578111	2.569719	0.874595
C	13.188217	2.008421	-0.247426
H	14.267671	2.067945	-0.352042
C	12.440480	1.368228	-1.228513
H	12.932768	0.939261	-2.095332
C	11.063271	1.271580	-1.089721
H	10.481516	0.762060	-1.853209
C	10.408288	1.811101	0.020286
C	13.430690	3.216664	1.954694
H	12.772306	3.802186	2.604511
C	14.093780	2.135126	2.818309
H	13.345680	1.474822	3.268113
H	14.686468	2.588512	3.618987
H	14.759889	1.517284	2.206759
C	14.487222	4.167955	1.382393
H	14.045140	4.909315	0.709849
H	15.253685	3.624645	0.821352
H	14.993377	4.698899	2.193655
C	8.898754	1.660425	0.136483
H	8.578127	2.130813	1.073242
C	8.174511	2.376050	-1.009910
H	8.433390	3.438202	-1.045966
H	7.090350	2.292372	-0.886641
H	8.436722	1.934279	-1.976718
C	8.499316	0.180999	0.192648
H	8.986909	-0.323180	1.032824
H	8.787752	-0.338408	-0.726917
H	7.415825	0.079880	0.309089

2.log

SCF (M062X) = -1440.74197617

E(SCF)+ZPE(0 K)= -1440.091488

H(298 K)= -1440.053353

G(298 K)= -1440.158676

Lowest Frequency = 23.2798cm-1

Al	9.249277	1.603083	2.935899
N	8.678595	2.752133	4.312451
N	10.083714	2.895939	1.861997
C	8.539592	4.064231	4.118807
C	8.997280	4.731454	2.970686
H	8.799942	5.793274	2.920060
C	9.795530	4.192649	1.950598
C	7.878080	4.892946	5.189159
H	6.818217	4.630751	5.259473
H	7.965471	5.955353	4.965860
H	8.324185	4.687306	6.165619
C	10.377520	5.132061	0.928585
H	10.085863	4.815161	-0.077348
H	11.470098	5.100517	0.965157
H	10.041352	6.153780	1.098873
C	8.287521	2.167818	5.571336
C	6.937780	1.854544	5.803229
C	6.600038	1.294060	7.038304
H	5.563677	1.038996	7.239363
C	7.566591	1.049971	8.001778
H	7.285464	0.617569	8.956675
C	8.901738	1.335824	7.736853
H	9.649377	1.109321	8.488350

C	9.295656	1.886631	6.516819
C	5.857505	2.049684	4.750582
H	6.272870	2.645988	3.931448
C	5.440890	0.693899	4.162729
H	6.285058	0.198437	3.678812
H	4.657810	0.833868	3.411358
H	5.046383	0.043388	4.950680
C	4.631029	2.784614	5.306176
H	4.897838	3.720198	5.807132
H	4.093897	2.165043	6.030906
H	3.934254	3.015454	4.495645
C	10.765121	2.159174	6.213181
H	10.943065	1.855800	5.175672
C	11.122470	3.646562	6.340682
H	10.591212	4.266366	5.613519
H	12.195359	3.787419	6.168609
H	10.890619	4.014492	7.346362
C	11.710368	1.325440	7.080440
H	11.452928	0.263853	7.044009
H	11.696535	1.652999	8.125544
H	12.735783	1.438199	6.719546
C	11.102943	2.441607	0.951424
C	12.429354	2.388517	1.417450
C	13.409105	1.909617	0.546916
H	14.440573	1.858711	0.884699
C	13.083756	1.485953	-0.735928
H	13.858784	1.111215	-1.396745
C	11.764875	1.532854	-1.168263
H	11.514325	1.187632	-2.167301
C	10.748398	2.009891	-0.337121
C	12.816055	2.818293	2.824575

H	11.914404	3.170618	3.339106
C	13.371592	1.635027	3.626588
H	12.635786	0.828954	3.690497
H	13.629632	1.961964	4.639970
H	14.283388	1.243932	3.162835
C	13.821000	3.976588	2.801118
H	13.437378	4.837590	2.245776
H	14.762247	3.670245	2.333506
H	14.046381	4.302871	3.821001
C	9.309673	2.018884	-0.826567
H	8.697808	2.539685	-0.082575
C	9.165989	2.757014	-2.162856
H	9.576382	3.770441	-2.117249
H	8.110949	2.826612	-2.442195
H	9.684554	2.225415	-2.966856
C	8.773309	0.586033	-0.942816
H	8.802760	0.074834	0.021940
H	9.364005	0.013569	-1.666048
H	7.733562	0.597970	-1.282662
F	10.370549	0.445462	3.467000
F	7.924681	0.884152	2.152092

3.log

SCF (M062X) = -3278.36924380

E(SCF)+ZPE(0 K)= -3277.071872

H(298 K)= -3276.998444

G(298 K)= -3277.173889

Lowest Frequency = 20.1815cm-1

Al	6.706209	2.674320	-0.043361

S	6.215253	4.316613	1.450237
N	8.554122	2.723199	-0.669015
N	6.818829	0.815713	0.515150
C	9.278225	3.962053	-0.829567
C	9.437833	4.509132	-2.115704
C	9.919883	4.516008	0.294588
C	9.236031	1.626361	-1.006281
C	7.683895	-0.050231	-0.018613
C	8.761111	0.323264	-0.823066
H	9.384419	-0.475157	-1.199165
C	7.558107	-1.524015	0.284342
H	7.561402	-1.710932	1.360444
H	8.372665	-2.078913	-0.178812
H	6.608734	-1.900955	-0.100804
C	6.524135	0.333687	2.885619
C	5.998860	0.290196	1.578471
C	9.757114	3.919446	1.684731
H	8.775793	3.441014	1.729761
C	10.278365	5.615853	-2.259672
H	10.413840	6.053858	-3.244222
C	4.775174	-0.341401	1.297685
C	10.769447	5.605567	0.093532
H	11.289660	6.039452	0.941162
C	2.958252	0.318562	-0.296880
H	2.160508	-0.079318	0.337366
H	2.620783	0.276816	-1.337973
H	3.119672	1.365344	-0.035146
C	8.744872	3.932788	-3.340853
H	8.358541	2.940091	-3.087511
C	10.626435	1.738946	-1.589928
H	10.584563	2.145287	-2.602705

H	11.097078	0.757432	-1.626617
H	11.248647	2.414862	-0.998832
C	10.959365	6.145831	-1.172754
H	11.625978	6.992173	-1.307454
C	4.058040	-0.886188	2.367704
H	3.099731	-1.360040	2.172960
C	7.554097	4.812843	-3.723119
H	6.838814	4.894685	-2.901329
H	7.028262	4.395807	-4.589057
H	7.899912	5.817264	-3.983449
C	5.791044	-0.261581	3.912088
H	6.185735	-0.248114	4.924698
C	7.879851	0.951781	3.197768
H	8.293262	1.361240	2.270272
C	4.236663	-0.497581	-0.115188
H	4.986856	-0.109137	-0.812463
C	4.562855	-0.862099	3.660329
H	3.999846	-1.310444	4.473350
C	9.682956	3.794822	-4.548365
H	9.939379	4.775837	-4.960294
H	9.183158	3.232313	-5.341877
H	10.620628	3.285766	-4.306743
C	3.940542	-1.965038	-0.462785
H	4.783896	-2.634377	-0.274294
H	3.668570	-2.047986	-1.519022
H	3.094128	-2.337117	0.123347
C	7.756708	2.104672	4.199626
H	7.151969	2.918891	3.787810
H	8.750622	2.496593	4.441311
H	7.297550	1.767785	5.135465
C	9.766387	4.987181	2.780561

H	10.755421	5.439585	2.907323
H	9.489102	4.537117	3.737473
H	9.040854	5.773657	2.555338
C	10.814059	2.841038	1.956329
H	10.699372	1.982105	1.286049
H	10.723262	2.473825	2.984575
H	11.824232	3.245988	1.828965
C	8.863011	-0.109692	3.708983
H	8.509761	-0.554936	4.644852
H	9.842048	0.340064	3.900468
H	8.999127	-0.916485	2.982649
Al	4.502052	4.731142	0.013406
S	4.998871	3.095812	-1.485085
N	2.758383	4.797560	0.870151
N	4.306936	6.496782	-0.794219
C	2.008680	3.600970	1.161768
C	2.096243	2.985881	2.422193
C	1.107341	3.144794	0.179018
C	2.149738	5.943549	1.184994
C	3.471013	7.422863	-0.319316
C	2.550919	7.192473	0.709066
H	1.978316	8.045183	1.044419
C	3.446860	8.810932	-0.918456
H	3.398916	8.768626	-2.009008
H	2.588212	9.365581	-0.542565
H	4.356860	9.355779	-0.658553
C	4.633800	6.562210	-3.222893
C	5.087737	6.910497	-1.936399
C	0.948453	3.840878	-1.165343
H	1.669125	4.663717	-1.214375
C	1.295166	1.864640	2.661574

H	1.364347	1.363198	3.623119
C	6.197077	7.754762	-1.747857
C	0.298749	2.049386	0.481845
H	-0.411201	1.691179	-0.259065
C	7.977420	7.333538	-0.052621
H	8.763139	7.579570	-0.772578
H	8.345224	7.572281	0.951342
H	7.791251	6.257839	-0.096876
C	2.979273	3.521156	3.537479
H	3.433552	4.457276	3.194985
C	0.921344	5.928096	2.062823
H	1.183303	5.557413	3.055893
H	0.508988	6.931470	2.158599
H	0.154495	5.259868	1.665234
C	0.394103	1.406395	1.710654
H	-0.234616	0.547522	1.925318
C	6.833040	8.267686	-2.881293
H	7.692409	8.920049	-2.756844
C	4.105783	2.538234	3.850317
H	4.682730	2.303830	2.954476
H	4.789693	2.961237	4.593830
H	3.695778	1.607301	4.252980
C	5.287958	7.121108	-4.322342
H	4.946448	6.881893	-5.324050
C	3.428091	5.657364	-3.428409
H	3.370704	4.979347	-2.573307
C	6.712070	8.132379	-0.367450
H	5.953022	7.861324	0.373618
C	6.370458	7.976898	-4.156982
H	6.863664	8.402385	-5.025615
C	2.184153	3.789970	4.824973

H	1.843422	2.850091	5.271031
H	2.824271	4.287287	5.559396
H	1.299459	4.411965	4.665997
C	7.011388	9.631960	-0.230397
H	6.185733	10.266673	-0.565260
H	7.224618	9.871862	0.815010
H	7.895477	9.910257	-0.812450
C	3.567535	4.773835	-4.669753
H	4.520980	4.238666	-4.654995
H	2.764845	4.031886	-4.687046
H	3.497487	5.351914	-5.597070
C	1.247600	2.892465	-2.330998
H	0.589973	2.016636	-2.307800
H	1.079122	3.406866	-3.283275
H	2.286597	2.549349	-2.299586
C	-0.453170	4.449792	-1.304552
H	-0.661317	5.168329	-0.506123
H	-0.547650	4.972351	-2.261349
H	-1.224432	3.673387	-1.268545
C	2.124890	6.465923	-3.472332
H	2.169269	7.231525	-4.255023
H	1.278295	5.805946	-3.691558
H	1.920899	6.960522	-2.516357

int3.log

SCF (M062X) = -1838.85273531

E(SCF)+ZPE(0 K)= -1838.201793

H(298 K)= -1838.161392

G(298 K)= -1838.272813

Lowest Frequency = 21.5551cm-1

Al	9.080853	1.644828	2.791200
N	8.701512	2.735363	4.282891
N	10.057394	2.912819	1.815491
C	8.616925	4.057299	4.131701
C	9.048524	4.745235	2.979557
H	8.866322	5.811034	2.960575
C	9.798422	4.216163	1.921615
C	8.033328	4.881136	5.250251
H	6.960048	4.683700	5.330290
H	8.185050	5.944234	5.068454
H	8.481336	4.605595	6.207981
C	10.314535	5.146938	0.856183
H	9.752029	4.963683	-0.066648
H	11.365029	4.952549	0.632205
H	10.189197	6.189818	1.145622
C	8.305266	2.128927	5.532363
C	6.946518	1.874883	5.781652
C	6.606040	1.296504	7.007804
H	5.562415	1.085787	7.222357
C	7.577449	0.976012	7.943742
H	7.293140	0.529399	8.891104
C	8.919884	1.200184	7.657924
H	9.672381	0.910754	8.382847
C	9.314009	1.766419	6.446169
C	5.857329	2.140496	4.754188
H	6.285899	2.717270	3.927988
C	5.355592	0.812559	4.169663
H	6.169548	0.256450	3.700545
H	4.594529	0.999132	3.406347
H	4.910904	0.194566	4.956982

C	4.683530	2.935626	5.339777
H	5.008040	3.858831	5.829442
H	4.137186	2.345054	6.081657
H	3.977175	3.198131	4.547338
C	10.785955	1.969075	6.115031
H	10.911656	1.751035	5.049103
C	11.233905	3.418382	6.347894
H	10.722257	4.119863	5.681791
H	12.309415	3.515528	6.163023
H	11.040666	3.720068	7.383240
C	11.701446	0.999673	6.864180
H	11.357695	-0.031402	6.747218
H	11.757061	1.234376	7.932531
H	12.716041	1.069873	6.462650
C	11.105072	2.427113	0.961405
C	12.413407	2.384503	1.488511
C	13.426530	1.883199	0.670441
H	14.445298	1.848252	1.044032
C	13.149803	1.416043	-0.610312
H	13.951517	1.023998	-1.227818
C	11.848336	1.436635	-1.093779
H	11.637404	1.050595	-2.086932
C	10.799822	1.941802	-0.320448
C	12.727562	2.882285	2.893165
H	11.783879	2.932721	3.447509
C	13.656647	1.933009	3.655175
H	13.247414	0.919496	3.682569
H	13.776922	2.286012	4.684642
H	14.655463	1.897589	3.208756
C	13.324230	4.296230	2.864277
H	12.630487	5.024887	2.436285

H	14.244453	4.313749	2.270569
H	13.567841	4.624012	3.879725
C	9.377484	1.921383	-0.853315
H	8.739581	2.468758	-0.151453
C	9.271841	2.605784	-2.220866
H	9.672746	3.623642	-2.195371
H	8.226212	2.654702	-2.537164
H	9.822090	2.050478	-2.986955
C	8.852851	0.481015	-0.924183
H	8.884210	-0.005093	0.054939
H	9.452228	-0.111816	-1.623522
H	7.814196	0.472392	-1.266061
F	7.615573	1.216317	2.034082
S	10.495800	-0.112491	3.089844
F	9.739499	-0.649160	4.498979

int4.log

SCF (M062X) = -3079.93131295

E(SCF)+ZPE(0 K)= -3078.631174

H(298 K)= -3078.556492

G(298 K)= -3078.735960

Lowest Frequency = 12.6596cm-1

Al	6.749357	2.040821	-0.894619
N	8.580337	2.514136	-0.733403
N	6.855446	0.476789	0.222567
C	9.140762	3.836951	-0.788611
C	9.426324	4.412200	-2.039293
C	9.492060	4.463440	0.417527
C	9.444059	1.493898	-0.834597

C	7.911791	-0.302725	-0.003441
C	9.085747	0.157471	-0.623240
H	9.851118	-0.585383	-0.806085
C	7.929478	-1.747198	0.436451
H	8.663395	-1.886298	1.234675
H	8.248058	-2.359709	-0.411421
H	6.956123	-2.093316	0.782496
C	6.161252	-0.028155	2.526001
C	5.848553	0.058351	1.155871
C	9.118789	3.851889	1.757759
H	8.255839	3.195102	1.587790
C	10.166336	5.595382	-2.058540
H	10.414662	6.054712	-3.010275
C	4.557492	-0.252218	0.674564
C	10.252532	5.633110	0.348702
H	10.565101	6.123042	1.265601
C	2.759491	-0.278928	-1.123624
H	2.289445	-1.232690	-0.857772
H	2.605793	-0.122584	-2.195022
H	2.252087	0.524234	-0.581912
C	8.922235	3.775760	-3.322857
H	8.754081	2.708698	-3.143689
C	10.886002	1.771203	-1.186985
H	10.948770	2.182415	-2.199644
H	11.472751	0.854814	-1.138599
H	11.320602	2.515013	-0.514486
C	10.609766	6.179755	-0.877413
H	11.208243	7.085210	-0.912139
C	3.579338	-0.602245	1.603693
H	2.575497	-0.826867	1.262946
C	7.568560	4.397621	-3.690144

H	6.831276	4.280730	-2.887557
H	7.159735	3.928546	-4.590850
H	7.687078	5.470142	-3.873034
C	5.142417	-0.392444	3.413421
H	5.365636	-0.459286	4.475082
C	7.552008	0.213308	3.101745
H	8.250222	0.425126	2.284877
C	4.256632	-0.288523	-0.817727
H	4.671279	0.607365	-1.288190
C	3.861627	-0.665489	2.964113
H	3.081035	-0.938241	3.668225
C	9.903032	3.909923	-4.490813
H	9.984695	4.947021	-4.831633
H	9.550289	3.316738	-5.338654
H	10.906941	3.563766	-4.224323
C	4.922001	-1.497797	-1.489250
H	6.011052	-1.441065	-1.438667
H	4.647745	-1.532239	-2.547297
H	4.592028	-2.428719	-1.014462
C	7.574493	1.422756	4.042206
H	7.349361	2.347416	3.506419
H	8.558854	1.520630	4.510684
H	6.836814	1.309183	4.843329
C	8.698206	4.907025	2.784520
H	9.532229	5.562564	3.056123
H	8.370126	4.412077	3.704698
H	7.868469	5.511903	2.407109
C	10.271465	2.987942	2.288015
H	10.462471	2.126042	1.640012
H	10.043025	2.612071	3.289100
H	11.191824	3.579397	2.350666

C	8.053427	-1.025475	3.861725
H	7.503455	-1.150851	4.799924
H	9.112158	-0.913414	4.114478
H	7.927508	-1.944374	3.284351
Al	4.603046	5.260853	0.325463
S	4.939536	3.300544	-0.640300
N	2.879830	5.201440	1.132140
N	4.197670	6.739716	-0.820840
C	2.283051	3.960349	1.545623
C	2.586279	3.422515	2.804407
C	1.391586	3.329024	0.660611
C	2.182818	6.321263	1.336661
C	3.309203	7.661187	-0.444922
C	2.448753	7.513394	0.656602
H	1.831194	8.365338	0.905178
C	3.186940	8.945520	-1.228960
H	3.134492	8.745752	-2.301669
H	2.300226	9.497025	-0.919214
H	4.067977	9.572349	-1.063304
C	4.575558	6.409784	-3.222280
C	4.966067	7.008692	-2.011229
C	1.055991	3.913976	-0.703955
H	1.721618	4.765895	-0.879999
C	1.971748	2.225162	3.173572
H	2.205522	1.780607	4.136691
C	6.048242	7.903064	-1.937603
C	0.783856	2.144129	1.081610
H	0.078278	1.644531	0.422430
C	7.765993	7.679655	-0.159882
H	8.588767	7.848347	-0.860299
H	8.088052	7.993016	0.838738

H	7.567186	6.604041	-0.124551
C	3.584693	4.099507	3.724278
H	3.742400	5.122599	3.366980
C	1.035615	6.304469	2.315443
H	1.404308	6.007894	3.303088
H	0.570425	7.287045	2.385306
H	0.282623	5.567601	2.026907
C	1.070073	1.594024	2.325559
H	0.592963	0.667840	2.632707
C	6.706566	8.234260	-3.124027
H	7.545459	8.923120	-3.092466
C	4.927637	3.368254	3.647190
H	5.307995	3.333711	2.619622
H	5.675658	3.866142	4.273100
H	4.811064	2.333661	3.988726
C	5.251259	6.789553	-4.383890
H	4.961517	6.355756	-5.335227
C	3.419614	5.423466	-3.281992
H	3.362468	4.922865	-2.311329
C	6.531976	8.464934	-0.610920
H	5.751969	8.312733	0.141163
C	6.296971	7.704261	-4.340714
H	6.808470	7.985637	-5.256065
C	3.094397	4.176160	5.173541
H	3.029241	3.182223	5.627225
H	3.793335	4.764422	5.774712
H	2.105709	4.640437	5.243128
C	6.852208	9.962693	-0.672528
H	6.023267	10.551301	-1.077741
H	7.077807	10.335538	0.330423
H	7.730817	10.156536	-1.295604

C	3.640026	4.323895	-4.322292
H	4.595841	3.818791	-4.154847
H	2.847225	3.575503	-4.241636
H	3.617092	4.712647	-5.345615
C	1.295050	2.903042	-1.829174
H	0.665874	2.014458	-1.710356
H	1.043285	3.352820	-2.795041
H	2.342909	2.587497	-1.852510
C	-0.386730	4.434559	-0.747387
H	-0.560046	5.214589	-0.000394
H	-0.607457	4.858159	-1.732233
H	-1.099036	3.623848	-0.560609
C	2.092444	6.157897	-3.513566
H	2.136844	6.757846	-4.429335
H	1.269805	5.442728	-3.617265
H	1.850127	6.823823	-2.678120
F	5.789460	5.768515	1.453104
F	6.641199	1.414392	-2.496878

SF2.log

SCF (M062X) = -597.793504381

E(SCF)+ZPE(0 K)= -597.788962

H(298 K)= -597.784677

G(298 K)= -597.813987

Lowest Frequency = 347.4353cm-1

S	-1.740008	0.902842	-0.373533
F	-1.845601	0.902842	-1.984223
F	-0.129318	0.902842	-0.267940

SF4.log

SCF (M062X) = -797.446212815

E(SCF)+ZPE(0 K)= -797.434574

H(298 K)= -797.428819

G(298 K)= -797.463025

Lowest Frequency = 216.4082cm-1

S	-1.770059	0.902842	-0.343661
F	-1.677515	-0.763805	-0.436152
F	-1.677515	2.569489	-0.436152
F	-1.925991	0.902842	-1.907505
F	-0.206304	0.902842	-0.186851

SF6.log

SCF (M062X) = -997.091208135

E(SCF)+ZPE(0 K)= -997.070211

H(298 K)= -997.063652

G(298 K)= -997.096969

Lowest Frequency = 339.2113cm-1

S	-1.771229	0.902842	-0.342312
F	-1.771229	-0.679290	-0.342312
F	-1.771229	0.902842	1.239820
F	-3.353361	0.902842	-0.342312
F	-1.771229	2.484974	-0.342312
F	-1.771229	0.902842	-1.924444
F	-0.189097	0.902842	-0.342312

TS1.log

SCF (M062X) = -2237.93906378

E(SCF)+ZPE(0 K)= -2237.277453

H(298 K)= -2237.233553

G(298 K)= -2237.353460

Lowest Frequency = -433.0549cm-1

Al	0.905325	0.412608	-0.087925
N	-0.394989	1.529514	0.890027
N	1.029408	1.770242	-1.519136
C	-0.603840	2.835261	0.711616
C	-0.120230	3.551398	-0.390840
H	-0.375283	4.601488	-0.437688
C	0.578520	3.022816	-1.483280
C	-1.436507	3.595619	1.716453
H	-2.489143	3.304534	1.644521
H	-1.357657	4.669159	1.547127
H	-1.112060	3.361018	2.733576
C	0.824331	3.928822	-2.664291
H	0.430560	3.471392	-3.576605
H	1.897885	4.070732	-2.821002
H	0.353968	4.900138	-2.515901
C	-1.139681	0.862315	1.927354
C	-2.495310	0.553928	1.683243
C	-3.215188	-0.092552	2.685134
H	-4.260214	-0.335008	2.523690
C	-2.608439	-0.457599	3.883361
H	-3.181510	-0.974208	4.646337
C	-1.269768	-0.169257	4.094480
H	-0.798181	-0.461561	5.028537
C	-0.511701	0.505729	3.130773

C	-3.136391	0.852562	0.335122
H	-2.669714	1.750427	-0.084296
C	-2.856780	-0.301491	-0.636787
H	-1.783337	-0.503025	-0.724627
H	-3.244248	-0.069730	-1.635368
H	-3.328289	-1.223872	-0.283346
C	-4.640028	1.123768	0.421130
H	-4.870756	1.887396	1.170234
H	-5.198976	0.218490	0.676189
H	-5.010824	1.469833	-0.547556
C	0.936498	0.849515	3.439233
H	1.337812	1.426382	2.598583
C	1.045137	1.731547	4.689673
H	0.447145	2.642496	4.592333
H	2.086080	2.021369	4.860111
H	0.698406	1.197672	5.579865
C	1.785797	-0.417918	3.592780
H	1.745223	-1.031577	2.689081
H	1.425783	-1.028473	4.427546
H	2.829844	-0.155567	3.790447
C	1.715417	1.307634	-2.696772
C	3.093052	1.559868	-2.843531
C	3.741577	1.047642	-3.967606
H	4.805488	1.225160	-4.094540
C	3.053108	0.306061	-4.920182
H	3.575818	-0.085451	-5.786796
C	1.697785	0.059547	-4.753914
H	1.164559	-0.531214	-5.493575
C	1.004846	0.548321	-3.643514
C	3.889894	2.320874	-1.795529
H	3.184671	2.824396	-1.126030

C	4.716419	1.342401	-0.949802
H	4.076532	0.594461	-0.470830
H	5.270565	1.876541	-0.171779
H	5.437192	0.810826	-1.579898
C	4.795482	3.393965	-2.410248
H	4.239064	4.068940	-3.067545
H	5.602369	2.947060	-2.998768
H	5.260369	3.990318	-1.620171
C	-0.472346	0.223075	-3.485439
H	-0.847819	0.753445	-2.602868
C	-1.293104	0.701049	-4.688687
H	-1.159206	1.772262	-4.865608
H	-2.357273	0.511735	-4.518625
H	-1.004486	0.171659	-5.602108
C	-0.668363	-1.281517	-3.255716
H	-0.123063	-1.624447	-2.370382
H	-0.302967	-1.853566	-4.114896
H	-1.727308	-1.519321	-3.114800
S	-0.629385	-3.249422	0.960188
F	-1.889209	-2.441789	1.585193
F	0.122836	-3.194347	2.397000
F	0.125590	-1.745989	0.489246
F	0.617079	-4.077873	0.335021
F	-1.396675	-3.324616	-0.475544
F	-1.313412	-4.621305	1.381263

TS2.log

SCF (M062X) = -2038.30024359

E(SCF)+ZPE(0 K)= -2037.646086

H(298 K)= -2037.603698

G(298 K)= -2037.719676

Lowest Frequency = -402.4344cm-1

Al	10.303808	1.503627	3.623757
N	9.102787	2.768459	4.580233
N	10.611060	2.863895	2.207040
C	9.007155	4.083920	4.377466
C	9.574999	4.744419	3.282268
H	9.407730	5.810990	3.217870
C	10.270460	4.149612	2.220924
C	8.222682	4.919213	5.360859
H	7.165866	4.634936	5.353142
H	8.305886	5.979633	5.125296
H	8.590013	4.744017	6.376362
C	10.645389	5.025512	1.050793
H	10.254797	4.599899	0.121936
H	11.733295	5.072079	0.942713
H	10.255953	6.035068	1.176967
C	8.307072	2.180032	5.622364
C	6.969374	1.839653	5.328439
C	6.237566	1.153938	6.298476
H	5.208738	0.875299	6.095407
C	6.807962	0.817299	7.524733
H	6.226151	0.274640	8.262980
C	8.118458	1.181723	7.801514
H	8.559442	0.916643	8.758099
C	8.889565	1.876446	6.863181
C	6.347322	2.203048	3.986647
H	6.841185	3.110976	3.623519
C	6.593441	1.105052	2.945434
H	7.656095	0.849668	2.868973

H	6.245430	1.431098	1.958724
H	6.073155	0.183908	3.220665
C	4.851570	2.513519	4.086675
H	4.642811	3.249694	4.868883
H	4.267010	1.613865	4.301038
H	4.491524	2.912174	3.134237
C	10.310636	2.285879	7.213867
H	10.691426	2.910128	6.397714
C	10.345865	3.129331	8.494831
H	9.682825	3.997217	8.428322
H	11.362191	3.487291	8.682670
H	10.037680	2.539984	9.363885
C	11.229650	1.065446	7.347986
H	11.240093	0.468612	6.431864
H	10.887110	0.408976	8.154021
H	12.251432	1.386228	7.574325
C	11.309702	2.339288	1.063538
C	12.710901	2.459304	0.990794
C	13.367137	1.884283	-0.097954
H	14.448378	1.959619	-0.167284
C	12.663393	1.208529	-1.087598
H	13.192184	0.766245	-1.925650
C	11.283637	1.093714	-0.995238
H	10.736682	0.555556	-1.764518
C	10.581976	1.649379	0.077523
C	13.518963	3.146882	2.080180
H	12.828882	3.714969	2.712789
C	14.208531	2.100214	2.965937
H	13.480031	1.414269	3.409977
H	14.767685	2.584485	3.772441
H	14.909972	1.503729	2.373188

C	14.548831	4.131095	1.514231
H	14.089934	4.853476	0.832433
H	15.339058	3.610674	0.964738
H	15.027230	4.683308	2.328017
C	9.073131	1.474742	0.151018
H	8.705986	2.030123	1.021341
C	8.374254	2.049387	-1.086711
H	8.626510	3.103136	-1.237375
H	7.288418	1.968796	-0.978648
H	8.658940	1.504117	-1.992050
C	8.708298	-0.003211	0.342554
H	9.161526	-0.411009	1.252472
H	9.061496	-0.601115	-0.503946
H	7.623650	-0.127421	0.416440
S	8.371914	-1.494018	5.605723
F	9.323656	-0.333164	4.672294
F	9.050553	-2.792928	4.992904
F	9.636087	-1.478393	6.734032
F	7.309575	-1.542451	4.275413

TS3.log

SCF (M062X) = -1838.64872188

E(SCF)+ZPE(0 K)= -1838.000523

H(298 K)= -1837.960088

G(298 K)= -1838.071515

Lowest Frequency = -378.6808cm-1

Al	10.833324	1.681103	3.954227
N	9.315513	2.740453	4.736406
N	10.693327	2.800812	2.291024

C	9.156144	4.043735	4.511106
C	9.706696	4.696398	3.402168
H	9.526459	5.759885	3.322154
C	10.328369	4.077123	2.300663
C	8.359163	4.872489	5.491737
H	8.178372	5.875241	5.104850
H	8.926074	4.953670	6.426060
H	7.405000	4.401870	5.736973
C	10.581660	4.936999	1.084929
H	10.254058	4.427381	0.175452
H	11.654147	5.124923	0.977870
H	10.065924	5.892893	1.171272
C	8.430905	2.074123	5.635772
C	7.250275	1.516749	5.088262
C	6.404613	0.796862	5.936844
H	5.491879	0.363565	5.539898
C	6.724459	0.609850	7.278444
H	6.061144	0.038821	7.919981
C	7.892124	1.158563	7.794106
H	8.139093	1.002971	8.840582
C	8.763762	1.896944	6.990051
C	6.885205	1.736623	3.625972
H	7.815506	1.948451	3.089360
C	6.234821	0.514415	2.973636
H	6.869737	-0.372201	3.056316
H	6.061563	0.714803	1.911992
H	5.260295	0.284498	3.416265
C	5.973477	2.962108	3.467924
H	6.466914	3.881245	3.793581
H	5.056487	2.838000	4.054200
H	5.692999	3.089810	2.417628

C	10.048570	2.445777	7.584545
H	10.534380	3.065033	6.822260
C	9.777481	3.323683	8.812287
H	9.063198	4.122304	8.591324
H	10.707369	3.779493	9.164024
H	9.368449	2.732271	9.637595
C	11.007262	1.302406	7.941604
H	11.229395	0.687206	7.064907
H	10.566528	0.656539	8.708718
H	11.948859	1.700481	8.331860
C	11.298242	2.248898	1.110982
C	12.660970	2.478617	0.844148
C	13.214499	1.905648	-0.303977
H	14.265671	2.068891	-0.523890
C	12.450129	1.125045	-1.157620
H	12.896993	0.690795	-2.046158
C	11.114359	0.879900	-0.860446
H	10.533661	0.244948	-1.520146
C	10.516909	1.420357	0.278737
C	13.560639	3.273306	1.778816
H	12.932411	3.779156	2.520033
C	14.501790	2.327419	2.537939
H	13.937259	1.586557	3.110670
H	15.134780	2.891530	3.230112
H	15.152835	1.794757	1.836566
C	14.376870	4.341348	1.039330
H	13.748818	4.987338	0.418853
H	15.125313	3.883822	0.385146
H	14.912109	4.969044	1.757408
C	9.059356	1.130452	0.612331
H	9.004716	0.957130	1.693739

C	8.155276	2.325326	0.275616
H	8.367666	3.194226	0.904865
H	7.102836	2.060446	0.423220
H	8.283618	2.615155	-0.773190
C	8.526905	-0.132444	-0.067121
H	9.185341	-0.988054	0.104952
H	8.413974	0.006650	-1.147641
H	7.539849	-0.376628	0.334503
S	8.781175	-1.105702	5.031449
F	9.599133	-0.010633	3.841028
F	9.828347	-2.312984	4.731657

TS4.log

SCF (M062X) = -3079.73054308

E(SCF)+ZPE(0 K)= -3078.432911

H(298 K)= -3078.358289

G(298 K)= -3078.537474

Lowest Frequency = -308.1656cm-1

Al	6.305703	3.098785	-0.686534
N	8.250944	3.035880	-0.968946
N	6.235684	1.320612	0.052499
C	9.016172	4.244177	-1.118296
C	9.180470	4.807180	-2.395813
C	9.608240	4.811018	0.026833
C	8.863714	1.891746	-1.249577
C	7.105888	0.379018	-0.330801
C	8.274709	0.634502	-1.050289
H	8.862926	-0.226424	-1.336877
C	6.905988	-1.058587	0.095084

H	7.410181	-1.720899	-0.609850
H	5.854472	-1.334103	0.167236
H	7.356500	-1.209160	1.081011
C	5.615277	0.720260	2.345831
C	5.241281	0.905635	1.002376
C	9.455317	4.163457	1.397484
H	8.502143	3.619913	1.411988
C	9.954348	5.966397	-2.504861
H	10.086836	6.424651	-3.480935
C	3.942850	0.618473	0.539957
C	10.382689	5.960672	-0.136053
H	10.851486	6.417096	0.729853
C	2.083427	0.847953	-1.167988
H	1.580283	-0.103160	-0.957909
H	1.896875	1.092778	-2.217005
H	1.629020	1.622315	-0.544140
C	8.541651	4.198568	-3.634443
H	8.140768	3.215273	-3.373194
C	10.270753	1.894317	-1.800154
H	10.713971	0.902394	-1.716362
H	10.905038	2.620299	-1.288843
H	10.244669	2.174224	-2.857492
C	10.556406	6.535796	-1.390817
H	11.156878	7.433923	-1.496236
C	3.011729	0.151359	1.470086
H	1.995308	-0.055876	1.154728
C	7.363271	5.055121	-4.100308
H	6.629173	5.200925	-3.301793
H	6.850639	4.577052	-4.941371
H	7.719923	6.036233	-4.426459
C	4.653851	0.224547	3.229644

H	4.917842	0.070945	4.272460
C	7.010291	1.045281	2.863412
H	7.671061	1.212926	2.004783
C	3.587954	0.754982	-0.935694
H	4.026066	1.689060	-1.306480
C	3.364744	-0.055859	2.799528
H	2.626418	-0.431573	3.501970
C	9.546111	4.036298	-4.783424
H	9.847333	5.009696	-5.183861
H	9.087624	3.475504	-5.602857
H	10.456879	3.513534	-4.476347
C	4.158135	-0.386924	-1.790911
H	5.247105	-0.359232	-1.853984
H	3.774449	-0.301276	-2.811762
H	3.849187	-1.360801	-1.393522
C	6.992532	2.337313	3.691349
H	6.646032	3.186753	3.096619
H	7.998005	2.558109	4.068105
H	6.324865	2.227437	4.553722
C	9.422213	5.185478	2.536233
H	10.408321	5.629800	2.707104
H	9.119341	4.694445	3.465471
H	8.709115	5.988391	2.327740
C	10.548931	3.115780	1.647453
H	10.480407	2.284511	0.939892
H	10.451729	2.703133	2.657378
H	11.543001	3.567093	1.555898
C	7.602706	-0.093909	3.703897
H	7.078724	-0.192687	4.659785
H	8.652840	0.114618	3.928743
H	7.546015	-1.060697	3.196061

Al	3.510081	4.921963	-0.458280
S	6.357856	4.805074	0.860822
N	1.734735	5.237200	0.356986
N	3.437311	6.685243	-1.382453
C	1.029189	4.101921	0.886450
C	1.374026	3.586012	2.146371
C	-0.018933	3.547345	0.121759
C	1.154656	6.431098	0.513961
C	2.548693	7.650028	-1.153432
C	1.562421	7.581471	-0.156876
H	0.973864	8.473680	0.006630
C	2.493003	8.872422	-2.046279
H	2.064368	8.576263	-3.010550
H	1.851137	9.634245	-1.604065
H	3.474555	9.297471	-2.254676
C	4.017209	6.595640	-3.771396
C	4.357974	6.963107	-2.458550
C	-0.437457	4.170704	-1.203761
H	-0.171681	5.232588	-1.177294
C	0.720399	2.430144	2.584535
H	0.995620	1.999426	3.543840
C	5.512889	7.715342	-2.175560
C	-0.658906	2.409163	0.611456
H	-1.461960	1.956788	0.037983
C	7.442439	7.838443	-0.562740
H	8.021089	8.621446	-1.065947
H	7.693523	7.873322	0.502481
H	7.763209	6.868206	-0.950855
C	2.372182	4.289176	3.050630
H	2.675171	5.218570	2.560656
C	-0.060350	6.551855	1.402932

H	0.132726	6.096702	2.377368
H	-0.332097	7.598000	1.540031
H	-0.911622	6.019595	0.966472
C	-0.276991	1.837681	1.822434
H	-0.775685	0.941862	2.179864
C	6.254002	8.203362	-3.253864
H	7.134203	8.810064	-3.061835
C	3.632680	3.451767	3.270069
H	4.061324	3.115183	2.321204
H	4.392260	4.042682	3.792392
H	3.408982	2.564896	3.871653
C	4.801052	7.090757	-4.815777
H	4.551341	6.829675	-5.840102
C	2.853600	5.663545	-4.061624
H	2.228902	5.614262	-3.162064
C	5.935072	8.031915	-0.748494
H	5.431604	7.321174	-0.088047
C	5.884542	7.922873	-4.563906
H	6.467212	8.319769	-5.389764
C	1.740454	4.647645	4.402859
H	1.474188	3.746403	4.964493
H	2.451954	5.217044	5.008000
H	0.832512	5.247534	4.290274
C	5.517454	9.444245	-0.316355
H	4.431064	9.548134	-0.247309
H	5.933815	9.671597	0.669671
H	5.891239	10.193649	-1.023546
C	3.389515	4.253143	-4.351162
H	4.028997	3.882347	-3.542038
H	2.560701	3.551894	-4.501148
H	3.991627	4.265033	-5.267255

C	0.328449	3.546013	-2.375528
H	0.047238	2.494653	-2.495735
H	0.101624	4.072908	-3.309167
H	1.412027	3.583063	-2.212938
C	-1.946485	4.087094	-1.449949
H	-2.515656	4.471834	-0.598333
H	-2.212249	4.672990	-2.334283
H	-2.269805	3.058111	-1.634922
C	1.963522	6.152430	-5.208120
H	2.494674	6.133625	-6.164780
H	1.091917	5.498452	-5.309604
H	1.607851	7.173599	-5.040587
F	4.601781	5.410755	1.062279
F	5.801067	3.044432	-2.333527

4. References

1 C. Cui, H. W. Roesky, H.-G. Schmidt, M. Noltemeyer, H. Hao and F. Cimpoesu, *Angew. Chem., Int. Ed.*, 2000, **39**, 4274–4276.
2 C. Bakewell, A. J. P. White and M. R. Crimmin, *Angew. Chem., Int. Ed.*, 2018, **57**, 6638–6642.
3 V. Jancik, M. M. Moya Cabrera, H. W. Roesky, R. Herbst-Irmer, D. Neculai, A. M. Neculai, M. Noltemeyer and H.-G. Schmidt, *Eur. J. Inorg. Chem.*, 2004, **2004**, 3508–3512.
4 G. C. Sati, J. L. Martin, Y. Xu, T. Malakar, P. M. Zimmerman and J. Montgomery, *J. Am. Chem. Soc.*, 2020, **142**, 7235–7242.
5 M. Stender, B. E. Eichler, N. J. Hardman, P. P. Power, J. Prust, M. Noltemeyer and H. W. Roesky, *Inorg. Chem.*, 2001, **40**, 2794–2799.
6 D. A. Saulys, J. Castillo and J. A. Morrison, *Inorg. Chem.*, 1989, **28**, 1619–1624.
7 D. Mulryan, A. J. P. White and M. R. Crimmin, *Org. Lett.*, 2020, **22**, 9351–9355.
8 V. Otero, D. Sanches, C. Montagner, M. Vilarigues, L. Carlyle, J. A. Lopes and M. J. Melo, *J. Raman Spectrosc.*, 2014, **45**, 1197–1206.
9 E. G. Palacios, G. Juárez-López and A. J. Monhemius, *Hydrometallurgy*, 2004, **72**, 139–148.
10 K. C. Pande and R. C. Mehrotra, *Zeitschrift für Anorg. und Allg. Chemie*, 1956, **286**, 291–295.
11 G. C. Hood and A. J. Ihde, *J. Am. Chem. Soc.*, 1950, **72**, 2094–2095.
12 C. Cui, H. W. Roesky, H. Hao, H.-G. Schmidt and M. Noltemeyer, *Angew. Chem., Int. Ed.*, 2000, **39**, 1815–1817.
13 J. Feldman, S. J. McLain, A. Parthasarathy, W. J. Marshall, J. C. Calabrese and S. D. Arthur, *Organometallics*, 1997, **16**, 1514–1516.
14 Y. Yang, T. Schulz, M. John, A. Ringe, H. W. Roesky, D. Stalke, J. Magull and H. Ye, *Inorg. Chem.*, 2008, **47**, 2585–2592.
15 J. A. Gladysz, V. K. Wong and B. S. Jick, *Tetrahedron*, 1979, **35**, 2329–2335.
16 K. Kawabata and H. Goto, *J. Mater. Chem.*, 2012, **22**, 23514–23524.
17 M. J. Frisch, G. W. Trucks, H. B. Schlegel, G. E. Scuseria, M. A. Robb, J. R. Cheeseman, G. Scalmani, V. Barone, B. Mennucci and G. A. Petersson, Gaussian 09; Revision D.01, Gaussian Inc., 2009.
18 Y. Zhao and D. G. Truhlar, *Theor. Chem. Acc.*, 2008, **120**, 215–241.
19 J. Tomasi, B. Mennucci and R. Cammi, *Chem. Rev.*, 2005, **105**, 2999–3094.
20 S. Grimme, J. Antony, S. Ehrlich and H. Krieg, *J. Chem. Phys.*, 2010, **132**, 154104.
21 K. Fukui, *Acc. Chem. Res.*, 1981, **14**, 363–368.
22 C. E. Dykstra, *Theory and applications of computational chemistry : the first forty years*, Elsevier, 2005.
23 R. Dennington, T. Keith and J. Milliam, GaussView 5.0, Semichem Inc., Shawnee Mission, KS, 2009.
24 E. D. Glendening, J. K. Badenhoop, A. E. Reed, J. E. Carpenter, J. A. Bohmann, C. M. Morales, C. R. Landis and F. Weinhold, NBO 6.0, Theoretical Chemistry Institute, University of Wisconsin, Madison, 2013.
25 M. P. Mitoraj, A. Michalak and T. Ziegler, *J. Chem. Theory Comput.*, 2009, **5**, 962–975.
26 F. Neese, *WIREs Comput. Mol. Sci.*, 2018, **8**, e1327.
27 F. Neese, F. Wennmohs, U. Becker and C. Riplinger, *J. Chem. Phys.*, 2020, **152**, 224108.
28 J.-D. Chai and M. Head-Gordon, *J. Chem. Phys.*, 2008, **128**, 84106.
29 J.-D. Chai and M. Head-Gordon, *Phys. Chem. Chem. Phys.*, 2008, **10**, 6615–6620.